HHS Public Access

Author manuscript

ACS Nano. Author manuscript; available in PMC 2023 May 11.

Published in final edited form as:

ACS Nano. 2022 August 23; 16(8): 11619–11645. doi:10.1021/acsnano.2c04337.

Future of Digital Assays to Resolve Clinical Heterogeneity of Single Extracellular Vesicles

Renee-Tyler T. Morales,

Department of Bioengineering, School of Engineering and Applied Sciences, University of Pennsylvania, Philadelphia, Pennsylvania 19104, United States

Jina Ko

Department of Bioengineering, School of Engineering and Applied Sciences and Department of Pathology and Laboratory Medicine, Perelman School of Medicine, University of Pennsylvania, Philadelphia, Pennsylvania 19104, United States

Abstract

Extracellular vesicles (EVs) are complex lipid membrane vehicles with variable expressions of molecular cargo, composed of diverse subpopulations that participate in the intercellular signaling of biological responses in disease. EV-based liquid biopsies demonstrate invaluable clinical potential for overhauling current practices of disease management. Yet, EV heterogeneity is a major needle-in-a-haystack challenge to translate their use into clinical practice. In this review, existing digital assays will be discussed to analyze EVs at a single vesicle resolution, and future opportunities to optimize the throughput, multiplexing, and sensitivity of current digital EV assays will be highlighted. Furthermore, this review will outline the challenges and opportunities that impact the clinical translation of single EV technologies for disease diagnostics and treatment monitoring.

Graphical Abstract

Corresponding Author: **Jina Ko** – *Department of Bioengineering, School of Engineering and Applied Sciences and Department of Pathology and Laboratory Medicine, Perelman School of Medicine, University of Pennsylvania, Philadelphia, Pennsylvania 19104, United States;* jina.ko@pennmedicine.upenn.edu.

Complete contact information is available at: https://pubs.acs.org/10.1021/acsnano.2c04337

The authors declare no competing financial interest.

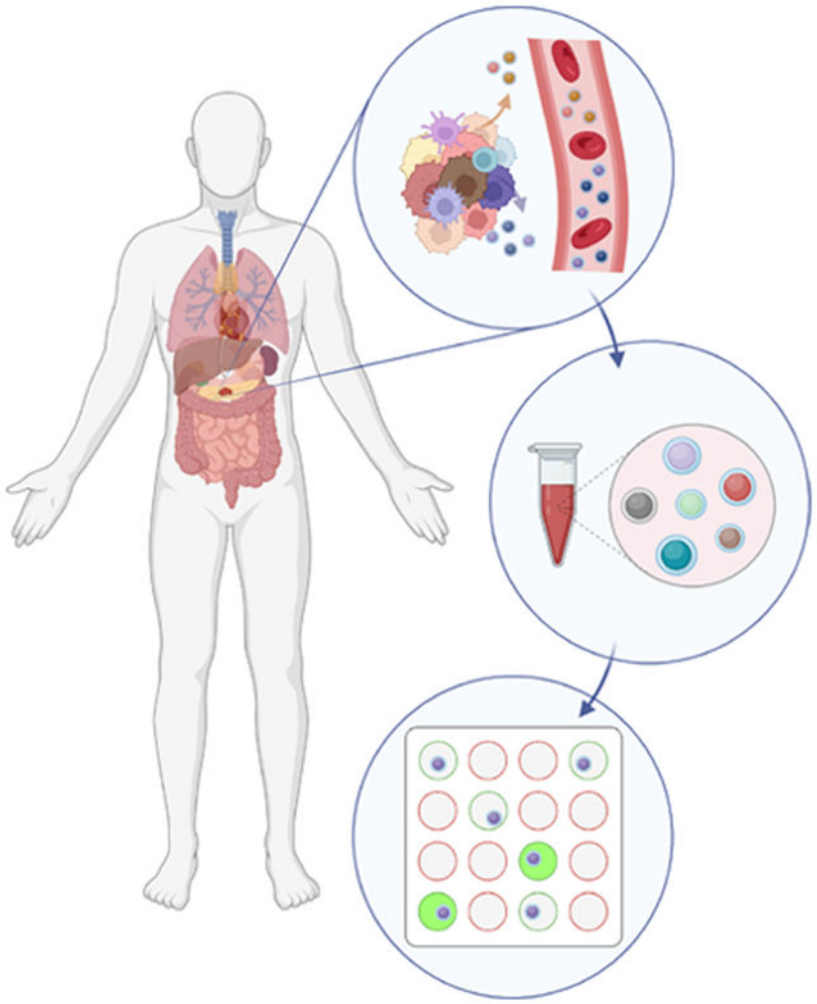

Keywords

extracellular vesicles; liquid biopsies; heterogeneity; digital assays; immunoassays; biomarkers; molecular diagnostics; multiplexing; point-of-care testing; clinical translation

Extracellular vesicles (EVs) are actively shed by cells existing in healthy and pathological states.[1,2] They are increasingly recognized as potential circulating biomarkers of disease.[1,3,4] To date, areas of precision medicine such as oncology increasingly rely on biopsied tumor tissue. However, sampling beyond the initial biopsy limits tissue immunohistochemistry's utility in navigating clinical management.[5] Recognizing the challenges and complications associated with core tissue resections, it is ideal to collect a circulating biomarker ("liquid biopsy") serially with a minimally invasive approach to monitor temporal changes in expression levels of key biomolecules. Notably, EVs exhibit high stability for protecting molecular cargo[6] as well as an abundance of sources. EVs are observed in most if not all biofluids, *e.g.*, blood,[7] sweat,[8] urine,[9] cerebrospinal fluid (CSF),[10] and saliva.[11] Biofluids carry varying quantities of EVs that shuttle diverse biomolecules from parental cells to recipient cells, including proteins,[12,13] messenger RNA (mRNA) fragments,[14] microRNA

(miRNA),[15] and DNA.[16] Thus, EVs are thought to be a cell's surrogate in intercellular communication[17] and studies have suggested EV markers are superior in sensitivity to cell-free DNA (cfDNA) for cancer diagnosis.[18,19] EVs participate in host immunity,[20] viral pathogenicity,[21] vascular diseases,[22] central nervous system (CNS) disorders,[23] and cancer.[24,25] Hence, EVs offer significant advantages to overhauling current limitations of diagnosis, prognosis, and monitoring treatment responses. EVs derived from cells can be used for therapeutic applications, but require EV characterization techniques to analytically validate or profile therapeutic cargo packaged in vesicles prior to deployment.[26–29] Many emerging methodologies and technologies may robustly and reliably parse the heterogeneity of different EV subtypes in healthy and diseased individuals.[30,31]

CHALLENGES WITH EV HETEROGENEITY

Impact of EV Heterogeneity on Diagnostic Sensitivity.

EV-based liquid biopsy has broad prospects for clinical applications. However, the complex heterogeneity of EVs remains to be the root of unresolved technical challenges (Figure 1). The molecular contents of EVs vary according to the organ source (*e.g.*, brain) and specific cell-of-origin (*e.g.*, neurons, microglia, astrocytes, oligodendrocytes).[32] Secreted EVs are quite heterogeneous between homogeneous or monoclonal cell populations,[33,34] and temporal expressions of analyte from a defined EV population can vary considerably.[35,36] Under the umbrella of EVs, the best studied classes are categorized by size: (i) exosomes (30–200 nm), (ii) microvesicles (<1000 nm), and (iii) apoptotic bodies (>1000 nm).[2,37,38] Other subsets include exomeres (<50 nm)[39] and large oncosomes (1–10 μm).[40] These EV subpopulations are all derived from distinct secretory mechanisms and subcellular compartments.[41] Furthermore, identifying disease-specific EVs in early stage cancers is difficult because of their scarcity beyond the background of EV shedding from healthy cells.[42] The stochastic nature of EV biogenesis and the rarity of molecular markers expressed in these nanometer particles renders bulk analysis challenging. This heterogeneity is also reinforced by the fact that nanoscale particulates (*e.g.*, protein aggregates, cell debris) that are carried in unfiltered clinical specimens overlap in size with EVs.[43] Therefore, bulk EV approaches are not suited to quantity the full spectrum of EVs, reflected by their large distributions in size.[44]

Furthermore, proteomic and transcriptomic signatures of different cell types can be partially reflected in their EV cargo but also differ substantially from those of their cells of origin, suggesting selective packaging of biomolecules in EVs.[45,46] The volume of EVs is approximately 10^6-fold smaller than that of a mammalian cell, limiting the packaging of molecular cargo and, thus, requiring large pools of EVs for analysis. The relative abundance of proteins expressed on or within individual EVs is markedly low[33] with an even scarcer number of mRNA[47] fragments and miRNA[47,48] packaged into single vesicles. As a result, EV proteins are profiled more often and protein composition defines the physiological behaviors of cells.

Taken together, these observations of multiparametric EV heterogeneity suggest that bulk EV analysis is insufficient to resolve the heterogeneity of individual EV subsets from clinical specimens. This is especially important in the context of potentially rare

pathological EV subsets in a bulk EV population. Hence, high-throughput single-EV or "digital" profiling methods can address these technical gaps to dissect the molecular contents of EV subsets. This review explores recent technical advances in employing such platforms as EV-based assays, proposes future opportunities to optimize the sensitivity, throughput, and multiplexing capacities of single EV methods, and highlights technical challenges and opportunities in translating and adopting such technologies for clinical practice.

DIGITAL EV ASSAYS

For digital assays, single target biomolecules or entities (*e.g.*, EVs, cells) are compartmentalized into single complexes with a Poisson distribution ($\lambda = 0.1$) to avoid multiplets.[49] Then analyte signals are "digitally" counted as single positive or negative detection events.[50] In contrast, analyzing target molecules in "bulk" is limited to analog measurements. The size of the signal decreases accordingly as the numbers of analyte are diluted, which often falls below detection limits. "Bulk" assays describe only the average of the overall molecular content of EVs. A critical prerequisite for digital detection is outnumbering the target molecule with an excess number of microcompartments. Each partition is randomly loaded with 0 or 1 target molecule according to Poisson statistics. Signals are then amplified *via* chemical or enzymatic reactions and reported by fluorescence within each complex. Such amplification methods have been paired with different partitioning methods (droplet microfluidics, microchambers, and nanostructures)[51] to discretely count and sum all single positive events for a more accurate concentration. Given the heterogeneity of EVs shed from healthy and diseased cells, designing a diagnostic method using a digital EV approach is necessary to generate a true reportable range and to better define clinically relevant cutoffs or thresholds.[52] Furthermore, digital EV assays can satisfy the required limit of detection (LOD)—the least amount of analyte that can be reliably detected on the reportable range—within subfemtomolar limits.

This discussion will survey five established groups of digital methods (Figure 2 and Table 1) for single EV analysis: antibody–DNA barcoding, ELISA (enzyme-linked immunosorbent assay), PCR (polymerase chain reaction), flow cytometry, and immunofluorescence imaging.

Antibody–DNA Barcoding.

By borrowing methods from single-cell RNA sequencing,[53] antibody (Ab)–DNA barcoding can increase the multiplexing and throughput of single EV analysis. This involves targeting proteins with Abs linked to oligonucleotides, converting protein identity to a DNA sequence that can be amplified for detection. Tian *et al.* described a labeling technique for single EV analysis that anchors DNA oligonucleotides on the EV membrane by conjugating a biocompatible anchor molecule (BAM) or Glypican-1 (GPC-1) Ab.[54] DNA-anchored EVs undergo digital PCR by being stochastically partitioned into microchambers, and two different DNA sequences are amplified *via* isothermal amplification to quantify the fraction GPC-1+ EVs from total EVs.

Ko *et al.* established an Ab–DNA barcode based single EV immunosequencing method (seiSEQ) that allows multiplexed protein measurements for single EVs (Figure 2A).[55] This

approach first models after previous work[56] with droplet microfluidics to compartmentalize and conjugate single EVs with Ab–DNA barcodes. Subsequently, DNA barcodes are sequenced to detect specific proteins at the single EV level. This study showcases an unlimited multiplexing capacity to profile large numbers of single EVs when coupled with deep sequencing.

Others have also exploited proximity ligation or extension assays to confer better specificity of protein identity *via* pairwise conjugation of proximal Ab–DNA probes. Wu *et al.* described a proximity-dependent barcoding assay (PBA) that uses Ab–DNA barcodes with rolling circle amplification (RCA) products to simultaneously profile 38 surface proteins on single EVs with next-generation sequencing.[57] Single EVs are labeled with PBA probes and are captured into microtiter wells. Oligonucleotides on PBA probes are brought together and anneal to form a RCA product with a complex nucleotide tag and sequence motif for DNA amplification. After amplification by PCR, DNA barcode information about surface protein composition on single EVs is reconciled by next-generation sequencing.

Digital ELISA.

In ELISA, target proteins are captured by Abs and incorporated with an enzymatic entity that catalyzes the formation of many thousands of molecules for signal amplification. Digital ELISA (dELISA) in the form of single molecule arrays (Simoa) was pioneered by Rissin *et al.* and has vastly improved measurement sensitivities by up to 1000-fold over traditional ELISA, enabling subfemtomolar detection of serum proteins.[49] Groups have now adopted these commercialized Simoa assays (Simoa, Quanterix) for digital EV detection.[58,59]

Particularly, Wei *et al.* adopted Simoa to purify tumor-derived EVs (EpCAM-CD63) and sort from universal EVs (CD9, CD63) to demonstrate superior diagnostic performance for colorectal cancer compared to serological biomarkers CEA and CA125.[60] Plasma EVs are first incubated with EpCAM or CD9 Ab-coated magnetic beads and then labeled with a biotinylated CD63 Ab and streptavidin-β-galactosidase (SBG). Bead EV immunocomplexes are confined into single microwells and a catalytic reaction between SBG and its substrate generates a fluorescent signal. Other compartmentalization techniques that have enabled digital assays include droplet microfluidics that can produce uniform droplets as low as the femtoliter scale in a high-throughput manner.[61]

Liu *et al.* combine droplet microfluidics and dELISA to discretely quantify breast cancer (BC)-derived EVs (droplet digital ExoELISA) with a LOD as few as ~10 exosomes per μL (~10^{-17} M) (Figure 2B).[62] Droplet digital ExoELISA resembles Simoa's capture scheme: BC-derived EVs expressing Glypican-1 (GPC-1) are immobilized onto paramagnetic microbeads through sandwich ELISA immunocomplexes tagged with an enzymatic reporter that produces a fluorescent signal. EV-bead immunocomplexes are then individually encapsulated into droplets for digital counting of BC-derived EVs. Similarly, Yang *et al.* similarly employed droplet dELISA by engineering a parallelized optofluidic system for a droplet-based EV analysis (DEVA) to profile single EVs from complex media in an ultra-high-throughput manner (~20×10^6 droplets/min) with a LOD of 9 EVs/μL.[63]

Droplet Digital PCR.

In recent years, digital detection has revolutionized not only the absolute quantification of proteins but also nucleic acids. Digital PCR (dPCR) follows basic principles of PCR but differs in quantification. In traditional quantitative PCR, target nucleic acids, along with PCR reagents and fluorescent probes, are amplified exponentially through a series of thermal cycles and fluorescence is monitored at each cycle. Meanwhile, dPCR involves partitioning individual nucleic acids into many replicate reactions resulting in 0 or 1 molecule across reactions. Following PCR, the concentration of template is determined by a Poisson distribution of the number of positive and negative amplified target reactions. However, since the discovery of "digital PCR" by Vogelstein and Kinzler,[64] it did not gain widespread use until later in 2007.[65] The lack of scalable and practical instruments for dPCR use delayed its initial adoption.

Now, commercialized droplet microfluidic technologies permit an exponential number of replicate reactions as droplets, making droplet dPCR (ddPCR, Bio-Rad) scalable and practical for routine use.[66,67] Chen *et al.* (2013) utilize two dPCR approaches—ddPCR and BEAMing[68] (beads, emulsion, amplification, magnetics) PCR—to interrogate single copies of mRNA from CSF-derived EVs for *IDH1* mutant DNA.[69] Both dPCR approaches comparably detect mutant *IDH1* mRNA in glioma patient-derived CSF EVs. Also, Allenson *et al.* describe that ddPCR analysis of single copy *KRAS* mutant EV DNA outperformed that of cfDNA for patients with pancreatic ductal adenocarcinoma (PDAC).[18]

Alternatively, Lin *et al.* developed a dual target aptamer detection probe (specific for EpCAM and PD-L1) to be paired with ddPCR (TRACER) for a quantitative proximity ligation assay (PLA) of PD-L1 expression on tumor-derived EVs (Figure 2C).[70] By leveraging the binding affinity of aptamers, specificity of proximity ligation, and sensitivity of ddPCR, TRACER enables an ultrasensitive quantification of PD-L1 expression in tumor-derived EVs. Unlike separate capture and detection probes for sandwich immunocomplexes, the proposed method is wash-free after aptamer incubation without interference from unbound aptamers. Following dual aptamer recognition, proximal aptamers are ligated and ddPCR can quantify ligation products. This in turn reflects, with high specificity, the number of PD-L1+ tumor-derived EVs for distinguishing cancer patients from healthy controls.

Flow Cytometry.

Flow cytometry involves measuring light scattering as single particles pass through a laser beam in sheath flow. Proteins from cells or EVs are detected with fluorescence using fluorophore-tagged Abs bound to the target. Flow cytometry is ideal for a multiplexed and high-throughput analysis based on its ability to examine multiple protein markers on thousands of cells per second.[71] However, bulk EV flow cytometry faces challenges of swarm detection. Conventional flow cytometry optics and fluidics are configured for microscale particles (*i.e.*, single cells) and not optimized for nanoscale EVs. As a result, EVs are likely to aggregate and be recognized as a single entity[72] and have required microbeads to capture multiple EVs for bulk analysis.[73] In contrast, specialized flow cytometers such as the Amnis ImageStream flow cytometer[74] have been developed to perform single EV analysis.

To optimize conventional flow cytometers for single EVs, groups have exploited DNA-based amplification techniques to increase the size of entities from nanoscale to microscale. For instance, Löf *et al.* developed a EV PLA (ExoPLA) that ligates two PLA probes to form a circular template that can be treated to RCA.[75] RCA products are labeled with a multicolor set of fluorophores to ensure strong detection signals and high specificity for protein targets. Meanwhile, Shen *et al.* developed a single EV flow cytometry technique that exploits DNA nanostructures that change conformation *via* a hybridization chain reaction (HCR) upon binding to CD63+ EVs.[76] Herein, authors designed a probe with an anti-CD63 aptamer, a domain to initiate HCR, and a flanked hinge sequence to achieve conformational change upon aptamer-target binding events. HCR products enlarge the overall size of single EVs and can bind to multiple fluorophores to amplify signals from low abundance marker molecules on EV surface.

Advances in optics have enabled flow cytometry for single EV analysis and the commercialization of nanoflow cytometry (NanoFCM) for profiling particle concentration, size distribution and EV surface protein makers.[77] This has stemmed from work by Tian *et al.*, which describes a high-sensitivity flow cytometer (HSFCM) for a multiparametric analysis (Figure 2D).[78] Compared to conventional flow cytometry, HSFCM achieved high sensitivity due to (i) reduction in probe volume to reduce background noise, (ii) slow flow rates for passing EVs in the laser beam channel, and (iii) high quantum yield from single-photon counting avalanche photodiode detectors. As a result, HSFCM is an ultrasensitive tool that allows single-particle enumeration (down to 40 nm) and surface marker profiling to identify EV subpopulations.

Immunofluorescence Imaging.

Immunofluorescence staining is compatible for large-scale multiplexing needs.[38,79] Lee *et al.* developed a single EV analysis (SEA) method to capture EVs and perform repeatable on-chip immunostaining and imaging (Figure 2E).[35] Biotinylated EVs are immobilized onto a neutravidin-coated glass surface of a microfluidic channel to perform recurring cycles of imaging for three different target markers for multiple rounds. EVs are labeled with many fluorescent Abs specific for several ubiquitous EV markers and tumor-derived EV markers, enabling a high degree of multiplexed molecular profiling (with concentration ranges of 10^7–10^{11} EV/mL).

Alternatively, He *et al.* developed a single EV assay that utilizes Total Internal Reflection Fluorescence (TIRF) microscopy to directly visualize and measure miRNA contents of single EVs from serum samples.[80] To accomplish this, DNAzyme probes and fluorophore-quenched substrates are delivered into EVs to activate a target miRNA-activated catalytic cleavage reaction that generates a fluorescent signal. Consequently, miRNA21 can be quantified for an *in situ* stoichiometric analysis of serum EVs. TIRF imaging suggests high-throughput and high multiplex potential.[81]

Cho *et al.* designed a multifluorescence single EV analysis by performing nanoparticle tracking analysis (NTA) platform to sequentially track scattering and fluorescence signals frame by frame.[82] The size and expression of membrane proteins (CD9, CD63, and CD81) of single EVs are analyzed by coupling NTA and TIRF.

Digital Assays Compatible for Single EV Detection.

Other digital assays can be compatible for single EV analysis. Particularly, this discussion will focus on dELISA. For instance, Akama *et al.* developed a droplet-free dELISA approach that is based on a tyramide signal amplification system.[83] On a bead immunocomplex, authors react a tyramide substrate with horseradish peroxidase (HRP) to produce short-lived radical intermediates. Tyramide radicals are then locally deposited on individual HRP-labeled beads to report fluorescence signals from localized bead enzyme reactions, and allow digital counting. Later, Akama *et al.* developed a wash- and amplification-free dELISA scheme (digital HoNon-ELISA).[84] Target antigens react with Ab-coated magnetic nanoparticles, and magnetic force draws targets into femtoliter-sized reactors. Within these reactors, capture Abs are anchored at the base to tether target antigen molecules, and the number of tethered particles is proportional to the target antigen concentration.

Although dELISA methods permit single molecule counting, low sampling efficiencies limit the number of target molecules that can be counted. Wu *et al.* developed a dropcast Simoa (dSimoa) to facilitate a higher sampling efficiency and simpler workflow.[85] Herein, authors form individual immunocomplex sandwiches of paramagnetic beads by coupling a biotinylated detection Ab and a streptavidin–DNA conjugate. Then RCA is performed to produce a long DNA concatemer on each immunocomplex with hybridized fluorophore-tagged DNA probes, allowing “on” and “off” beads to be counted by fluorescence imaging. Beads are then dropcast onto a microscope slide and allowed to air-dry to form a monolayer film. Similar to droplet dELISA,[79] dSimoa demonstrates up to a 25-fold enhancement in sensitivity (attomolar levels) over the gold standard Simoa. Wu *et al.* later readapted dSimoa’s signal amplification scheme for a flow cytometric readout (MOSAIC) to digitally count “on” and “off” events.[86] This approach first involves capturing single target molecules with an excess number of Ab-coated paramagnetic beads, where beads follow stochastic loading of either zero or one target molecule according to a Poisson distribution and then detected by flow cytometry. Taken together, MOSAIC’s flow cytometric readout demonstrates high-throughput and high multiplexing capacity to simultaneously measure a large number of analytes at femtomolar sensitivities.

FUTURE DESIGN OPPORTUNITIES FOR DIGITAL EV ASSAYS

The heterogeneity among EV subpopulations confounds the results of studies attempting to identify the functional roles of EVs in disease. There is a range of biogenesis mechanisms, different origins (specific organelles/cells/tissues), and biomolecular components. It is clear that classifying EV subtypes will require future technological advances (Figure 3) to optimize digital assays so they can characterize the molecular composition of individual EVs by balancing sensitivity, throughput, and multiplexing. The following techniques can be extended to digital EV assays to establish an integrated and continuous “lab-on-a-chip” workflow.

EV Enrichment.

The clinical potential of single EVs can only be truly defined once the range of EVs from a given source is fully described and isolated into their specific EV subsets. Traditional isolation methods rely on time-consuming, multistep protocols and require multiple instruments that make it unlikely to translate into diagnostics. To optimize EV yield, it is idealistic to perform all preparation steps on a single, integrated assay.

Physical Energy Field Modalities.—Techniques that exploit physical energy fields to separate cells (magnetic,[87,88] acoustic,[89,90] and dielectrophoretic forces[91,92]) are promising tools to manipulate nanoscale EVs.[93,94] They offer the versatility to handle many subpopulations of a complex sample and preserve the structural integrity of EVs, whereas classical isolation methods often alter the morphology, content, and functions of EVs.[95–97]

Particularly, Wu *et al.* reported a continuous-flow, acoustics-based separation method. This approach combines ultrasound standing waves and microfluidics (acousto-fluidics) to sort exosomes directly from undiluted whole blood samples using differential acoustic forces (Figure 3A, left).[7] By tuning the acoustic frequencies, micrometer blood cell components can be fractionated to derive cell-free plasma for downstream EV enrichment (with a purity of ~98% and a yield of ~82%). Nanoscale EVs can be efficiently segregated into subgroups of sizes from 100 μL of undiluted human blood within ~25 min. Finer size exclusion and segregation is necessary for downstream analysis as clinical samples may contain non-EV lipid particles and protein aggregates that share size similarities with EVs.

An alternative approach developed by Wan *et al.* exploits magnetic fields and lipid-based nanoprobes (LNPs) (Figure 3A, left).[98] LNPs are constructed with one end containing two PEGylated lipid tails that spontaneously insert into lipid membrane EV surface, while another end consists of biotin that binds to NeutrAvidin-coated magnetic beads. As a result, EVs derived from non-small cell lung cancer patient plasma samples can be isolated in ~15 min with a capture efficiency (~68%) similar to that of ultracentrifugation (varies from <10 to 70%[99]). By reducing the number of purification steps to a single-step process, LNPs can minimize the redundancies and damage imparted on downstream molecular analyses.[95] Although the nanoscale EVs are anchored onto magnetic beads *via* lipid insertion, there is a concern of how to reverse the labeling of these lipid probes for a traceless, downstream analysis of single EVs.

Nanopatterning Structures.—The ability of surface probes to interact with molecular targets for successful capture is fundamentally important for single EV analysis. The sensitivity of current biosensing interfaces is defined by boundary conditions, microscale mass transfer limits, and interfacial binding reactions.[100] To further improve the capture efficiency, various nanolithography approaches have been proposed to enhance microscale mass transfer to increase the probability of EV antigen-Ab collisions (*e.g.*, herringbone mixers[101]).

Work by Zhang *et al.* showcases a nanolithography-free approach that facilitates the self-assembly of colloidal arrays into a microfluidic chip to achieve a multiscale integration of 3D herringbone nanostructures (Figure 3A, middle).[102] This approach expands the available

surface area for EV affinity binding sites, drains boundary fluids to lessen fluid resistance, and enhances mass transfer for successful EV binding. As a result, this nanolithography-free approach enables a notably low LOD of 10 EVs per μL (200 EVs per assay) to detect low-abundance EV subpopulations from blood plasma. However, the success of EV capture is also dependent on the variable binding affinities of each EV surface protein marker.

Affinity Capture Probes.—To link measurements of EV molecular content to a specific disease, methods, for example, in early cancer diagnosis, can either detect rare, mutated proteins (*e.g.*, KrasG12D) or the coexpression pattern (*e.g.*, GPC1+/EGFR+/EPCAM+) of proteins.[103,104] Profiling multiplexed signatures of EV proteins, however, depends on the binding affinities of its Ab panel. Although Abs are pivotal linkers for label-based detection of target biomolecules, there are major challenges such as batch-to-batch variation among manufacturers and their processes as well as exorbitant costs. Researchers also need to be aware of Ab cross-reactivity[105] and nonspecific binding.[106] Ab cross-reactivity can limit the scaling of multiplexing and, thus, assay performance may read out inaccurate or even false conclusions. Moreover, nonspecific Ab binding to other targets is a large hurdle that requires optimizing protocols.[71] Aptamers and nanobodies are functional alternatives to Abs and are better suited for ultrasensitive EV detection since their sensing range matches the nanoscale size of EVs (Figure 3A, right).

Aptamers.—Notably, aptamers are single-stranded oligonucleotides that possess binding affinities comparable to or even higher than Abs and have become widely used as affinity capture probes in biosensing. Aptamers are artificially produced as well-defined, low variability products with long storage stability, providing a low cost and chemically modifiable alternative for biosensing.[107] Liu *et al.* described a method that utilizes aptamers and λ-DNA to both selectively sort EVs based on size classes and perform surface protein analysis of single EVs.[108] Also, He *et al.* developed an ultrasensitive single EV assay that can directly visualize and quantify tumor EVs from plasma using activatable aptamer probes that trigger fluorescence.[109]

Furthermore, controlling the binding affinities of aptamers for label-based cell sorting is a useful and versatile function for EV analysis as traditional Ab labeling is not easily reversible. Kacherovsky *et al.* designed a reversible cell-selection technology that employs magnetic beads coated CD8-binding DNA aptamers to capture and elute CD8+ T cells for a traceless isolation directly from peripheral blood mononuclear cells.[110] The efficiency of aptamer-mediated capture of CD8+ T cells were comparable to Ab-based CD8 magnetically activated cell sorting that is used clinically. Similarly, Gray *et al.* coated magnetic beads with EGFR-binding aptamers to reversibly isolate EGFR+ cells.[111] To retrieve label-free cells, cells are treated with an oligonucleotide complementary to the aptamer linker. The carrying-over of bead labels on a cell's surface can pose challenges during postsorting assessments like phenotyping by flow cytometry. For multiplexing purposes, aptamers demonstrate feasibility, versatility, and reversibility to the labeling process.

Although aptamers have distinct advantages over Abs, their availability for various receptors is limited compared to Abs. Generating highly specific aptamers has proven challenging with conventional processes like SELEX (Systematic Evolution of Ligands by EXponential

Enrichment).[112] Modern high-throughput screening platforms will be required to design and select aptamers for epitopes of multiplexed protein targets with optimal binding affinities.[113,114]

Nanobodies.—Since their discovery in 1993 by Hamers-Casterman's group,[115] nanobodies are considered functional alternatives over conventional monoclonal Abs (two heavy chains and two light chains). Derived from Camelidae, nanobodies are from the variable domain of variant heavy chain-only moieties and are devoid of light chains, reducing their size (~15 kDa).[116] Consequently, there is less steric hindrance between a protein of interest and label[117] and binding affinities comparable to Abs that allow greater spatiotemporal resolution for imaging[118] and multiplexing,[119] which can be scalable for single EV analysis.

Work by Guo *et al.* described a method that functionalizes organic electrochemical transistors with a monolayer of nanobodies specific for SARS-CoV-2 spike protein to distinguish against MERS-CoV-2 spike protein with an LOD as low in the attomolar range.[120] The sensing apparatus involves a self-assembled monolayer of spike-specific nanobodies linked with a fusion SpyCatcher protein, which is conjugated to a complementary SpyTag peptide. The SpyCatcher-SpyTag conjugate pair is attached to a functionalized alkylthiol layer on a gold electrode. As a result, this approach demonstrates high specificity and single-molecule sensitivity with human saliva and sera, has a fast sample-to-result time of 10 min, and requires a working sample volume of 5 μL.

However, a limitation of nanobodies is that they are predominantly made by immunizing camelids, requiring (i) lymphocyte isolation from peripheral blood, (ii) cloning variable regions of single domain Abs, and (iii) immune library preparation for phage display.[121] This process can lead to broad variations in binding affinity that signals a need for more synthetic nanobodies for more controllable characteristics.[122]

Signal Amplification.

To optimize signal detection for single EV analysis, several signal amplification techniques are available. Approaches to detect single EV proteins such as tyramide signal amplification[83] or enzyme-linked fluorescence[62] use enzymes to catalyze the deposition of fluorescent substrates near affinity capture probes. For this review, a majority of signal amplication methods focus on nucleic acid amplification techniques that are effective for gaining signals of DNA, RNA, or proteins conjugated with oligonucleotides.

Isothermal Amplification.—PCR is a gold standard, but requires dedicated instrumentation for temperature control. To resolve this, isothermal assays have been developed that allow amplification reactions to run at constant temperature. These include enzymatic-dependent methods such as RCA,[123,124] RPA,[125,126] and loop-mediated isothermal amplification.[127] A limitation of schemes like PCR, RPA, and LAMP is that they are exponential amplification techniques, which can systematically suffer from uneven amplification as error is exponentially amplified.

To avoid this, there are linear amplification methods that exist such as RCA, where enzymes (i) ligate DNA or RNA to form a circular oligonucleotide from a circular template or padlock probe and (ii) produce long DNA concatemers (Figure 3B, left).[128] As a result, groups have demonstrated that relatively large DNA nanostructures can form *in situ* on a solid support or complex surface (*i.e.*, EV membrane) upon target recognition and carry multiple binding sites for fluorophores to enhance visualization.[123,124] Furthermore, RCA can eliminate an extra reverse transcription step for RNA detection unlike other linear amplification methods like *in vitro* transcription[129] or isothermal methods such as RPA and LAMP. It is important to note that RCA amplicons can impose steric hindrance from the micrometer sized coiling of single stranded oligonucleotides and can limit multiplexing for extracellular protein analysis of intact nanoscale EVs. Altogether, a majority of isothermal amplification techniques are limited by relying on enzymatic activity.

As a result, a non-enzymatic, simple alternative of isothermal amplification for single EV analysis is HCR, which depends on hybridization alone. Upon initiation, a chain reaction of recognition and hybridization events between DNA hairpin molecules triggers the self-assembly of fluorophore-labeled hairpins into an elongated polymer on the surface of EVs (Figure 3B, left).[76,130] However, issues that arise are the limited functionality of the DNA scaffold for multiplexing and controlling the rate of HCR unlike enzymatic-dependent methods that use heat deactivation.

Multispectral Materials.—Optical multiplexing has a sizable impact on the label-based detection of EVs. Immunofluorescence imaging reports protein measurements by relying on fluorophore labels. However, existing materials are limited by an “optical multiplexing ceiling” due to spectral overlap. One commercial solution, Luminex, has circumvented this limitation by loading dyes into microspheres conjugated to target molecules with custom concentrations of fluorophores to create distinct color sets for multispectral visualization.[131] Due to photobleaching and prolonged exposure times, however, traditional fluorophores do not make ideal candidates for spectral multiplexing. Also, excess and free amounts of dye can influence signal detection by producing false positives and reducing signal-to-noise ratio. Therefore, multispectral materials must exhibit notable stability and tunability to optimize multiplexed signal detection (Figure 3B, right).

To address these challenges, Hu *et al.* synthesized a class of polyyne-based materials.[132] They were able to achieve 20 distinct Raman frequencies within a ‘carbon rainbow’ *via* systematic chemical modifications. Polyyne-based materials demonstrate high specificity, sensitivity and photostability with increasing color choices by increasing polyyne length. To establish spectral barcodes for optical multiplexing, polymer beads are loaded with different combinations of polyynes. Alternatively, Nguyen *et al.* developed MRBLEs (microspheres with ratiometric barcode lanthanide encoding) for spectral multiplexing.[133] The authors designed microspheres containing >1000 distinct ratios of lanthanide nanophosphors that can be distinguished *via* imaging and can measure protein/peptide binding affinities in high-throughput using small amounts of material. A current challenge, however, remains to be size matching with EVs as these beads are optimal for single cells. Therefore, downsizing the beads loaded with these multispectral materials to the nanoscale EV size range will be a promising strategy for multiplexing single EV analysis.

It is anticipated such multispectral materials and others (*e.g.*, quantum dots,[134] upconversion nanoparticles,[135] and carbon-based nanodots[136]) will provide abundant sources to address immunolabeling issues tied to fluorescent bleaching for a multiplexed analysis of single EV protein markers.

Signal Detection and Transduction.

To date, enzymatic target amplification processes such as PCR are routinely used for detecting disease-marking nucleic acids for clinical diagnosis.[137–139] Yet, preamplification can suffer many pitfalls to differing degrees that restricts the deployment of nucleic acid tests at point-of-care (POC) settings. Issues include but are not limited to enzyme instability and variety; nonspecific amplification; amplification errors and biases; poor multiplexing ability; operational speed and cost; lengthy and laborious sample preparation; and the dependence on instruments and trained personnel.[140] Furthermore, following the capture of single-molecule binding events from EVs, another vital challenge is how to transduce reported signals into observable readouts.

Nanopores.—Bypassing preamplification requirements, the following methods demonstrate high single-molecule sensitivity for digital analysis of EV molecular contents. Nanopores can detect many classes of analytes (DNA, RNA, and proteins) with label-free operation and single-molecule sensitivity.[141] Molecules are electrokinetically translocated by an externally applied electrical field through nanopores, resulting in temporal variations of measured ionic current (Figure 3C, left).[142,143] To selectively detect molecules, Cai *et al.* customized molecular probes (designed with a DNA carrier and a molecular beacon) to target and capture single miRNAs selectively in an electro-optical nanopore sensing system.[144] The authors accomplished femtomolar-level detection of miRNAs directly from unprocessed patient sera (volumes as little as 0.1 μL) and can profile a panel of three miRNAs of the same family (with a single nucleotide difference) for prostate cancer (PC) stage classification.

Similarly, He *et al.* developed a digital immunoassay using solid-state nanopores to quantify protein concentration.[145] The authors designed proxy and pairable DNA probes to link into dumbbell nanostructures after analyte binding *via* a magnetic bead-based sandwich assay. Thus, translocations dumbbells (“1”) or unpaired DNA (“0”) are classified as positive and negative events, respectively. As a result, electrical nanopores signals can be read out as a digital count of thyroid stimulating hormone concentration.

It is important to note the potential effects of nanopore size as the membrane pore diameter[146] as well as thickness[147] thins down: the measurement resolution increases. Thus, tuning solid-state nanopores offers a path for optimizing the signal-to-noise ratio of molecular translocation measurements, as compared to commercially available, biologically derived protein nanopores (*e.g.*, Oxford Nanopore Technologies). Once nucleic acid species are extracted, nanopore sequencing is underway in a matter of minutes, which is more suitable for POC applications that require fast turnaround times and no amplification. At its current state, nanopores are effective for short-read sequences such as mRNA and miRNA fragments packaged into EVs. However, issues remain, such as fast translocation times

of DNA molecules, which can be orders of magnitude too fast for current bandwidth of measurements.[143,148] Furthermore, reads are coalesced as multiple bases and cannot discriminate single bases,[149] unless a high-throughput fabrication of nanopore arrays with two-dimensional thickness can be achieved.

CRISPR.—Besides its broad use in gene editing, clustered regularly interspaced short palindromic repeats (CRISPR) can enable biosensors with high sensitivity and single-nucleotide specificity to fulfill needs in nucleic acid detection such as distinguishing miRNA isoforms or short/fragmented RNA species (Figure 3C, left).[150] For instance, Gootenberg *et al.* developed a SHERLOCK (specific high-sensitivity enzymatic reporter unlocking) that unites RPA with collateral cleavage by CRISPR/Cas13 to detect single RNA and DNA molecules with single-nucleotide sensitivity.[151] To enhance for multiplexing and portability, authors later combined Cas13 with Csm6 (a supporting CRISPR enzyme) and a lateral flow format to visually read out Dengue or Zika virus single-stranded RNA and mutations of patient liquid biopsies.[152] At present, a major limitation for CRISPR-based collateral cleavage for higher-order multiplexing is the requirement for preamplification to increase detection sensitivity.[152,153] Preamplification reactions usually need several hours and may cause amplification errors along the process.

CRISPR-based methods have emerged that do not require preamplification. CRISPR-Chip, developed by Hajian *et al.*, immobilizes a complex of CRISPR/Cas9 with a specific single-guide RNA onto a graphene field-effect transistor.[154] Following hybridization events of unamplified, whole genomic DNA and complementary guide RNA, the changes in graphene surface conductivity generate measurable signals that are read out on a portable reader with a LOD (low femtomolar range) and turnaround time of less than 30 min. Similarly, Bruch *et al.* relied on CRISPR/Cas13a to power their integrated microfluidic electrochemical biosensing platform for POC detection of microRNAs without the need for preamplification.[155] This work's biosensing principle relies on collateral cleavage by CRISPR/Cas13 and immobilization of RNA reporters labeled with biotin and FAM on the sensor surface. Coupled with glucose oxidation, formed H_2O_2 byproducts function as a surrogate for target miRNA and are amperometrically detected with an LOD of 10 pM within 4 h using small volumes (<0.6 μL).

Nanoplasmonics.—Nanoplasmonic platforms are scalable to match size ranges of EVs and utilize metallic nanostructures and nanoparticles to produce localized surface plasmons to increase the sensitivity and specificity of EV sensing (Figure 3C, right).[156]

Seminal work by Im *et al.* described a label-free, high-throughput nanoplasmonic EV assay that requires fabricating periodic nanohole arrays on a gold film deposited onto a glass substrate.[157] These nanohole structures focus the electromagnetic fields at each grating and, due to their 200 nm diameter and thickness, enable a probing depth of <200 nm to match size range of EVs. Furthermore, nanoholes are functionalized with Abs to enable shifts in plasmonic resonance upon binding of EV surface proteins and lysates. Others like Raghu *et al.* have developed 80 nm gold sensing elements functionalized for CD63+ EV capture to sit atop 90 nm diameter quartz nanopillars (total height of 490 nm) to not only reduce background noise from nonspecific binding to substrate but also resolve the detection limit

to a single EV.[158] As a result, an array of spatiotemporal plasmonic events from EV surface binding interactions can be captured and analyzed according to single nanopillars of interest. A major imitation of fabricating nanostructures is the requirement for state-of-the-art and low throughput nanofabrication technologies such as ion beam milling and electron beam lithography, which can lead to elevated fabrication costs. Popular techniques such as soft lithography are limited by their resolution to enable nanostructure patterning, giving rise to variable dimensions and thereby altering the optical resonance parameters to detect robust and reliable signals.

In addition to fabricated nanostructures, works like that of Liang *et al.* have implemented gold nanoparticles to enhance detection. Specifically, the binding of capture Ab-coated gold nanospheres and nanorods to EVs on a sensing interface generates local plasmons to directly capture and quantify tumor-derived EVs.[159] Min *et al.* adapted gold periodic nanohole arrays as a substrate to enhance fluorescent label detection with locally produced plasmons for a multiplexed profiling of EV protein markers with improved sensitivities.[160] However, it is important to keep in mind that plasmonic resonances can only enhance fluorescence in wavelengths that overlap with plasmonic resonances, which can limit multiplexing capabilities.

Electrical Interfaces.—Electrical interfaces confer high sensitivity, rapid response, excellent portability, and easy signal amplification for EV detection (Figure 3C, right).

Mathew *et al.* designed an electrochemical readout of tumor-derived EVs using nanoscale interdigitated electrodes (nIDEs).[161] The electrochemical sensing workflow combines a sandwich immunoassay and a double amplification scheme (alkaline phosphatase-based enzymatic amplification and electrochemical amplification *via* redox cycling on nIDEs). As a result, authors achieve an LOD as low as 5 EVs/μL and a reporter range that spreads over six orders of magnitude (10–10^6 EVs/μL) using PC cell lines.

Another electrical detection method that may be compatible for EVs is electromechanical detection. Wang *et al.* assembled an electro-mechanical apparatus for rapid, amplification-free, and ultrasensitive detection of SARS-CoV-2 RNA from unprocessed nasal swabs of COVID-19 patients.[162] The authors constructed a double-stranded DNA tetrahedral base linked to a flexible single-stranded DNA cantilever with an aptamer tip probe (with complementary oligo-nucleotides) that specifically binds to analyte. These units are immobilized onto a liquid-gated graphene field-effect transistor, such that mechanical perturbations are transduced into electrical signals from target-probe binding. As a result, authors were able rapidly detect ultralow concentrations of SARS-CoV-2 RNA from unprocessed biofluids in a matter of 4 min.

A major limitation of traditional electrical interfaces is that complex biofluids can passivate electrodes, limiting their longterm usage and sensitivity. As a result, they are susceptible to false-positive results. To tackle this, electrical sensing interfaces need to implement antifouling strategies (*e.g.*, bovine serum albumin[163]) to enhance their robustness for transducing signals for molecular detection.

Signal Analysis.

In the past decade, single-cell profiling techniques have evolved to a point where researchers can describe the diversity, interrelationships and plasticity among cellular phenotypes[164] as exemplified by Argelaguet and colleagues.[165] Scaling smaller than single cells, EVs are being investigated at a multiomics level (Figure 3D, left).[166,167] To disentangle the heterogeneity of EVs, experimental platforms are needed to not only isolate EVs into single units for analysis, but also describe as much of the diverse molecular contents packed into EVs.

Single-Cell Multiomics: Parallel Transcriptomics.—Modeling and coupling techniques from single-cell profiling may enable the collection of in-depth information[168] of EV cargo. For example, Macaulay *et al.* created a single-cell genome and transcriptome sequencing (G&T-seq) protocol that physically separates genomic DNA and polyadenylated RNA *via* biotinylated oligo(dT) primers, permitting bisulfite conversion of DNA without altering the transcriptome.[169] Subsequently, the genome and transcriptome are amplified in parallel and sequenced. In contrast, Dey *et al.* worked on a genomic DNA-mRNA sequencing (DR-Seq) method that selectively incorporates promoter sequences into cDNAs to allow selective amplification of cDNAs over genomic DNA *via in vitro* transcription.[170] Furthermore, by adding a sodium bisulfite treatment step before PCR amplification of genomic DNA fractions, Angermueller *et al.* established a method for a genome-wide, parallel single-cell methylome and transcriptome sequencing (scM&T-seq).[171] Major challenges that exist for capturing transcriptomic information in single EVs include the sparse abundance of RNA copies as well as the lack of polyadenylated sequences of EV RNA fragments that is common in single-cell RNA transcripts for capture and readout.

Single-Cell Multiomics: Parallel Proteomics.—The physical separation of cell lysate of a single cell can enable simultaneous multianalyte measurements of proteins and RNAs. Darmanis *et al.* used a lyse-and-split strategy to establish parallel workflows to quantify expressions of protein (with a proximity extension assay followed by qPCR) and mRNAs (with quantitative reverse transcription PCR).[172] Meanwhile microfluidic- and sequencing-based approaches such as CITE-seq[173] and REAP-seq[174] have exploited Ab–DNA barcodes to jointly measure surface protein levels and mRNA transcripts in single cells. Although expansive in terms of multiplexing, these methods can be fundamentally challenged by high background due to nonspecific binding of Abs. Others like Albayrak *et al.* have addressed these limitations by introducing digital PLA (dPLA), which combines PLA and ddPCR to digitally count single copies of mRNA and proteins from single cells.[175] Later, Lin *et al.* parallelized 144 single-cell dPLA assays into an integrated microfluidic platform (μ-dPLA), which enhances the LOD of dPLA by up to 55-fold.[176] To ease multianalyte measurements of protein and RNA for single EVs, a simplified and unified workflow is necessary to address the digital detection of biomolecules from a single EV.

Single Organelle Omics: Mitochondrion.—Diving deeper than single cells, subcellular organelles (including EVs) are compartmentalized with diverse, dynamic, and specialized functions that requires sensitive technologies to study their subcellular biology. Requirements to study subcellular organelles center on the ability to sense and parse out

desired organelles according to individual features (*e.g.*, size and molecular composition) and high-throughput operation to sample sufficient entities from single cells.[177]

Classical techniques such as differential centrifugation[178] mask any endogenous heterogeneity of individual mitochondrion as an averaged pool. To analyze mitochondria at a single-organelle resolution, nanofluidic isolation approaches have been proposed.[179,180] Following isolation, single-organelle methods have attempted to sequence DNA. Morris *et al.* isolated single mitochondrion *via* micropipette aspiration and analyzed whole genomic DNA to identify mitochondria variants within a single cell, without loss of spatial origin.[181] Although authors were able to amplify the full genome using specific primers and nested/seminested PCR and construct sequencing libraries, the laborious isolation steps call for more high-throughput methods to handle single organelle samples. MacDonald *et al.* described a nanoscale, multiparametric approach for single mitochondrion isolation and analysis *via* fluorescence-activated mitochondria sorting (FAMS).[182] Once labeled and lysed from diverse tissues/cell lines, functional single mitochondrion can be isolated and analyzed in a flow cytometry fashion by size, membrane polarization status, or protein markers. The authors demonstrated FAMs-based isolation enables direct profiling of proteomics and mtDNA copy number at the level of individual mtDNA molecules within a single mitochondrion. Yet this method sacrifices capturing subcellular spatial information about the organelle at a low throughput to a high-throughput analysis *via* single organelle sorting with no spatial context.

Single Organelle Omics: Nucleus.—Cell nucleus isolates are viable alternatives to scRNA-seq as they can be derived from fresh or frozen tissues from biobanks, have sufficient RNA for accurate prediction of cell expression levels, and are free of artifacts from dissociation of difficult tissues (*e.g.*, nervous tissue[183] and skeletal muscle[184]).[185] Habib *et al.* developed DroNc-seq—a massively parallel single nucleus RNA-sequencing method that combines single nucleus RNA sequencing (sNuc-seq) and Drop-seq[186] to profile nuclei at low-cost and high-throughput.[187] As a result, authors were able to profile tens of thousands of nuclei from mouse and human biobanked brain samples to produce cell atlases. Others like Gaublomme *et al.* demonstrated a multiplexing approach for sNuc-seq that employs Ab–DNA barcodes to distinctly label nuclei.[188] Once pooled, labeled nuclei are incorporated into droplets for sNuc-seq DNA barcodes contain a polyA tail that couples the same bead barcode to its nucleus of origin, significantly improving throughput and cost. Although DNA barcoding strategies are advantageous for multiplexing, they do carry issues with universal tagging. McGinnis *et al.* addressed these issues by developing a MULTI-seq protocol that uses lipid-tagged indices for single-cell and single nucleus RNA sequencing.[189] The authors determined that lipid- and cholesterol-modified oligonucleotides are reagents suited for universally barcoding any lipid-based membrane bound organelle. However, this remains to be a challenge when performing single organelle analysis with multiplets, where each organelle must be sorted from sister organelles of the same mother cell.

Artificial Intelligence.—To supplement single EV analysis, it is expected machine learning algorithms may be necessary to process the wealth of molecular data and recognize patterns (Figure 3D, right).[190] Unlike classical “big” datasets for machine learning, current

EV-based liquid biopsies have “small” dataset sizes ranging on the order of tens to hundreds. However, it has been demonstrated that multiplexed EV signatures can be classified by machine learning algorithms and disease diagnosis and staging can be predicted from small datasets.[191,192]

Machine learning utilizes algorithms to analyze data and subsequently learn and make informed decisions from that data. Instead of relying on a single machine learning algorithm, groups have constructed an ensemble of algorithms (including linear discriminate analysis, logistic regression, naive Bayes, K-nearest-neighbors, and support vector machines which can all be elaborated in more detail here[190]). Yang *et al.* built upon a previous machine learning-based liquid biopsy approach[193] for staging PDAC that combines several algorithms to analyze a multianalyte panel of tumor-derived EV mRNA/miRNA, cfDNA, KRAS mutation, and CA19-9 protein markers.[194] Each classifier model will overfit data differently and thus average out results to provide a more accurate model than any single method alone. As a result, the model can also detect PDAC (84% accuracy) prior to metastasis and compared to imaging alone, demonstrating proof-of-principle that an ensemble machine learning approach can preoperatively screen patients amenable for surgery.

Meanwhile, deep learning structurally layers algorithms to establish an artificial neural network that can learn and make autonomous decisions. Shin *et al.* applied deep learning into a Raman spectroscopy (SERS) analysis of circulating EVs to diagnose stage I lung cancer.[195] The authors derived correlations of SERSs signals from lung cancer cell line- and patient plasma- derived EVs using a residual neural network (Resnet)-based deep learning model. In essence, Resnet depends on building a shortcut connection by tagging previous input to the output to preserve previous gradient information, resolving any issues of a vanishing gradient related to deep architecture. Following training, plasma-derived EVs of stage I lung cancer patients were evaluated in a test set, and the deep learning model predicted lung cancer diagnosis correctly with ~91% of patient samples.

A fundamental limitation for executing these machine learning and deep learning models in EV-based liquid biopsies is that there is a considerably large data requirement for training sets to avoid overfitting. As a result, current small-plex and bulk EV analyses may be rendered unsuitable. That, however, does not discount their effectiveness in single EV analysis. There is high dimensionality when teasing apart the molecular heterogeneity of single EVs and longitudinally capturing multiplexed measurements over the course of disease progression and treatment.

ROADMAP FOR THE CLINICAL TRANSLATION OF DIGITAL EV METHODS

Analyzing shed EVs allows for a minimally invasive capture of complex molecular information in cells, which can fulfill precision medicine efforts for diagnosing and treating patients without an invasive biopsy. However, bringing digital EV assays into the clinical realm requires overcoming roadblocks in clinical translation. Technological advances in all areas of the workflow—(i) understanding the biological variables of EV measurements; (ii) standardization of clinical sample acquisition and optimization of EV enrichment; (iii)

integration of digital detection and data analysis—are needed to (iv) clinically validate single EV assays for disease diagnosis, prognosis, and treatment monitoring (Figure 4). Furthermore, cases studies will also be discussed of how single EV technologies that have been used to study cancer can also be applied to various acute and chronic diseases, with a focus on CNS disorders.

Biological Considerations for EV Measurements.

Mapping EVs to Parent Cell of Origin.—It is thought that the pathological capacity of EV molecular cargo is mapped by their cell of origin and represents, to a certain degree, the state of the parent cell. However, conventional methods sub-optimally sort out EVs from bulk cell populations. As a result, it is difficult to discretely map the secretion of specific, or rare, EV subsets to their parent cell of origin. These challenges can be exemplified in intratumoral heterogeneity,[196] where cell subpopulations harbor different genetic and transcriptional profiles for distinct biological functions.[197,198] The coexistence of different cell clones within the same tumor has significant implications for clinical management. For instance, a number of clones may dominate the tumor composition, whereas minor subclones, that are often below detection thresholds, can determine the clinical course of progression and recurrence.[199] In combination with single-cell approaches, single EV analysis could determine varying EV subsets derived from single-cell clones[200] as they may rely on different biogenesis mechanisms and package cargo with different quantities and types of molecular content.[201,202] Methods that either characterize single EVs from bulk cells or bulk EVs from single cells mask the inherent differences of quantity and phenotypes of EV secretions between cells. The ability to stoichiometrically relate specific subsets of EVs to their parent cell would be useful for addressing current limitations in single EV analysis. Even within the same source organ, different cells release batches of EVs that are packaged with different biomolecules. Due to this complexity, there are needs and opportunities for single-cell, single-EV mapping to profile the packaging of single EVs and trace shedding from single parent cells of the same source organ rather than evaluating EVs with a bulk analysis.

Microfabrication techniques have enabled the direct capture of single cells and subsequently, cell-specific secretions.[203,204] Established approaches to capture and characterize single-cell EV secretions have used microchamber arrays and a spatially resolved Ab barcode readout[205] or pneumatic valves to trap and culture single cells and immobilize secreted EVs for immunostaining and fluorescence microscopy.[34] Most recently, hydrogel-based microparticles or “nanovials” have been exploited to be suspendable and sortable microwells for capturing single cells and their secretions together.[206,207] Nanovials may also be suitable for capturing and later collecting cell clone-specific EVs for downstream molecular analysis. Methods that optically report the biogenesis of single EVs[208] from single parent cells would be useful for single-cell-single-EV mapping. For example, cell transfection with fusion constructs of a fluorescent protein and an EV-specific marker (*e.g.*, CD63[209,210]) or transfection with a membrane-targeted fluorescent protein[211] can contribute to a workflow for interrogating EV subsets from parent cells. There are growing efforts to trace cell-free biomolecules (*e.g.*, cell-free RNA) to their parental cells/tissue of origin based on omics

approaches such as transcriptomics profiles.[212,213] Similarly, the ability to map EVs to their parental cell by aligning EV genomic[214] or proteomic[215] profiles to parent cells.

EV Disease Kinetics.—EV-based liquid biopsies show promise for the early detection and management of diseases such as cancer. However, a major challenge is the scarce presence of biomarkers in biofluids that cannot be readily augmented,[216] precluding early detection. To address these issues, mathematical models have predicted the time window for early cancer detection available based on the kinetics of blood biomarker shedding from early tumors. Hori and Gambhir extrapolated from mathematical models that a tumor can grow undetectable for the first decade and advance to a volume of ~20 mm^3 before detection with current blood tests.[217] Mathematical models of blood biomarker samples describe that detecting and distinguishing aggressive (2 month doubling) and nonaggressive (18 month doubling) tumors can be as early as ~7 months and ~9 years prior to clinical imaging, respectively.[218]

Several factors dilute the number of tumor-derived EVs including but are not limited to tumor-derived EV shedding rates, host cell EV production, and clearance rates and, therefore, impact the diagnostic requirements of molecular EV markers. Patient tumors do not always express positive biomarkers, and protein shedding rates can vary by as much as 4-fold magnitude for cells of the same tumor type.[219] Furthermore, the background shedding from healthy host cells can confound the fleeting amount of biomarker shedding from dying or dead cells. Bulk EV analysis (*e.g.*, standard ELISA) requires ~10^4–10^6 EVs per sample to reliably detect abundant EV markers.[220] Ferguson and Weissleder generated computational models to predict the thresholds of tumor detection for various EV-based detection assays. Current bulk EV measurements are suited more for assaying large tumors (~10 cm^3) and are ~10^4-fold insensitive to detect early stage lesions (~1 cm^3).[42] In contrast, single EV methods (*e.g.*, SEA[35]) are predicted to detect early stage tumors in humans as small as 1×10^{-5} cm^3 (10 μg or about 10,000 tumor cells).

EV Markers.—To address challenges in EV enrichment, identifying universal EV markers would enable the study of particular EV subpopulations and their functions in health and disease. Traditionally, researchers have used tetraspanins CD9, CD63, and CD81 as ubiquitous EV biomarkers and immunoaffinity methods relying on these proteins to purify EVs and define their molecular composition.[33,221] However, Kugeratski *et al.* report tetraspanin markers CD9, CD63, and CD81 mirror their expression pattern in the parental cells, which may explain why tetraspanins levels are heterogeneous in EVs from distinct cell types.[13] This study establishes a comprehensive proteomic atlas of core EV proteins and identified syntenin-1 as a majorly abundant core EV protein found in different cell, biofluid, or species sources. Furthermore, bona fide biomarkers are needed to distinguish different classes of EVs produced by different biogenesis pathways. Recent work by Mathieu *et al.* has suggested CD9, CD63, and CD81 tetraspanin markers on EVs formed from intraluminal vesicles of endocytic compartments (exosomes) or at the plasma membrane (ectosomes) are expressed mutually but differently.[222]

Standardization.

Several studies have reported advances in single EV methods and EV biomarkers, but validation has been hampered by regulatory challenges. More attention is needed on the processes of biomarker discovery and validation to allow the successful implementation of single EV assays for clinical use. Only standardized protocols of preanalytical steps (sample acquisition and preparation) and quantification, as well as transparency in reporting, can ensure a meaningful and reliable catalog of biomarker signals that are not misperceived as noise. Lack thereof results in a method that is not reproducible for clinical use.

Preanalytical Steps.—Downstream analysis is affected by variations and quality of sample handling and processing.[223] It is worth noting that disease-specific EV biomarkers can be outnumbered by a million-fold excess of nontarget species. Therefore, interferants in the sample can drastically influence the analytical specificity of single EV assays.[52] When searching for rare EV subsets within complex media, researchers need to take precautions and troubleshoot interference factors—non-EV and EV components—from clinical specimens. For example, flow cytometry results can be perturbed by nonspecific binding of particles from plasma, limiting the fluorescence detection of rare EVs.[224] Lipoproteins and protein aggregates overlap with the size range, composition, and morphology of EVs.[225,226] Moreover, influences from sample processing like hemolysis and platelet contamination all interfere with single EV analysis.[52] EV isolation strategies separate and concentrate EVs variably and nonspecifically. Better EV isolation methods are needed to not only subtract contaminations from analyte but also sort disease-relevant EVs from other host EVs. Classical methods of EV capture and characterization suffer from poor EV isolation efficiency and purity, long processing times, and operational costs that make it increasingly unfeasible for clinical—especially POC applications.[227] Thus, optimizing EV enrichment modules in assays to achieve high recovery and specificity (as discussed previously), as well as standardizing the acquisition and handling of clinical specimens, can minimize systematic errors during biomarker characterization.

Quantification.—Quantification is a critical element for translating single EV methods and biomarkers for clinical use. Although techniques are progressing toward ultrasensitive detection limits,[228] normalizing measurements significantly varies from one laboratory setting to another. Normalizing quantities of EV molecular analytes (proteins, nucleic acids, lipids) to the original sample volume, original EV number concentration, or total amount of EV molecules can serve as a valuable index for EV diagnostics.[229] Research groups have already begun developing referencing standards for EV and EV-molecule quantification by incorporating “spike-in” recombinant vesicles into their methods.[74,230,231] Ideally, EV reference materials should share physical and biochemical attributes of EVs, controllability over surface molecular expression and interior cargo, and be distinguishable from sample EVs to support device calibration and biomarker quantification.

Reporting.—Lastly, it is important to disclose single EV methods with the same rigorous standards with which they are developed. The EV biology field needs more transparent methods reporting to allow reproducibility for other cohorts. To do so, the EV-TRACK consortium has established a knowledgebase and a coaching tool to promote transparency

and reproducibility for methods.[232] The International Society of EVs (ISEV) has also recommended that each preparation of EVs is to be, at minimum, defined by (i) quantitative measures of the source of EVs (*e.g.*, volume of biofluid), (ii) abundance of EVs, as well as screenings for coisolated components (iii) associated with EV subtypes and (iv) nonvesicular particles.[223] To assist researchers in reducing non-EV interferants, many non-EV proteins observed in past studies using immunoaffinity-based capture have been cataloged into an available repository.[233] Furthermore, web-based compendia like Exo-Carta[234] and Vesiclepedia[235] feature manually curated catalogs of characterized EV molecular cargo (RNA, proteins, lipids, metabolites) from several studies to enable research queries.

Commercialization.

The approval process of regulatory bodies—Clinical Laboratory Improvement Amendments (CLIA) and the United States (U.S.) Food and Drug Administration (FDA)—ensures optimal, sequential, and standardized methods but has impacted the commercialization of single EV assays for use in the clinical realm. As of now, there is no FDA approved EV platform that is approved for clinical use. To commercialize and adopt EV-based assays for clinical use as laboratory developed tests (LDT) or *in vitro* diagnostics (IVD), stakeholders must comply with rules and regulations for rigorous analytical and clinical validation.[236]

EV-Based Laboratory Developed Tests.—Single EV assays can be marketed as a LDT (in the form of a service or kit) after obtaining FDA premarket regulatory clearance. The caveat, however, is that LDTs are designed, validated, and manufactured exclusively for in-house use in a clinical laboratory. In the U.S., the FDA does not regulate LDTs. CLIA regulates laboratory testing, requires clinical laboratories to be certified by the Center for Medicare & Medicaid Services, and ensures that clinical laboratories conduct rigorous analytical and clinical validation of LDTs.[237] Then laboratories can run assays on human specimens to determine information about diagnosis and prognosis or monitor treatment responses and disease burden.

EV-Based In Vitro Diagnostics.—Alternatively, single EV methods can be marketed as assays for distribution as IVDs, which can be purchased from the manufacturer for POC use in professional settings (clinics or laboratories) or resource-limited settings (rural areas or patient homes). IVD products are defined by the FDA as “reagents, instruments, and systems intended for use in diagnosis of disease or other conditions, including a determination of the state of health, in order to cure, mitigate, treat, or prevent disease or its sequelae”.[238] FDA-approved EV analysis and markers can be sold as IVDs (in the form of complete kits) for their specified purpose after obtaining premarket regulatory clearance for analytical and clinical validation from the FDA. IVDs would include all protocols and controls to perform a test independently in diverse settings with relatively less training and still obtain accurate, reliable, and reproducible clinical results.

Progress in Regulatory Approval.—Researchers have used Simoa (Quanterix)[60] and Droplet Digital PCR (BioRad),[69] commercial instruments for single-molecule analysis, as assays for single EV analysis, but these commercial instruments have not been approved by regulatory agencies for that context of use. As of now, the first bulk EV-based, CLIA-

validated, and commercially available test to become available is the ExoDx Prostate IntelliScore (EPI Test, Bio-Techne) for PC.[239,240] In 2019, the EPI Test received a groundbreaking FDA breakthrough device designation to expedite the FDA's regulatory review process. This noninvasive urine test is used to screen for 3 EV mRNA (*ERG*, *PCA3*, and *SPDEF*) alongside standard of care tests to distinguish benign/low-grade PC from high-grade PC for men (age >50 years) with a PSA level of 2–10 ng/mL ("gray zone") presenting for an initial biopsy. EPI scores are correlated to high-grade PC and have been prospectively validated at a cut off score of 15.6 for reducing unnecessary biopsies. Thus, all patients whose score is >15.6 will proceed with the recommended clinical course (including a core tissue biopsy). The EPI Test has received strong enthusiasm by stakeholders as demonstrated by the National Comprehensive Cancer Network guidelines and the draft Medicare Coverage Determination to support urologists' decision making to defer or proceed with a core tissue biopsy. This is critical given the notable risks of complication after transrectal ultrasound-guided prostate biopsies.[241]

Since the EPI test is determining the necessity of a prostate biopsy, it can be suggested that core tumor biopsies may demonstrate considerable progression to high-grade (>grade group 2) PC[242] that may limit treatment options. Individually profiling EVs can better resolve the heterogeneity to identify rare targets or subtype-specific molecular information, which is analogous to benefits of single-cell approaches as bulk cell analysis is limited. Therefore, single EV analysis may allow patients to be amenable to earlier diagnosis and actionable treatment as early stage developing tumors are volumes well below detection thresholds[42,104] (as discussed previously) of current standard of care tools.

Clinical Feasibility: Point-of-Care Principles for Commercialization.

Although single-molecule digital assays have gone through commercialization, further work is needed in areas such as multiplexing, throughput, cost, and ease of use to entice clinical stakeholders for investing and adopting such technologies for single EV analysis. If there is one lesson that the past few years of the coronavirus disease 2019 (COVID-19) pandemic has stressed: there is an ever-growing clinical need for robust and reproducible diagnostics, comparative testing methods, faster approval by federal agencies, and rapid production of tests to meet supply and demand.[243] End users especially do not need platforms that require multiple operation steps, prolonged turnaround times, low-throughput, expensive and bulky equipment, and labor-intensive protocols. Therefore, single EV assays are more likely to be commercialized and implemented for clinical use by following design principles of POC testing and balancing high analytical performance with low system complexity.[244] These resources also have to be made accessible to wider communities and commensurate with central laboratory findings from the clinic.

Rapid Turnaround Times.—Single EV assays need to be amenable for high-throughput operations to allow versatility for treating diseases with differences in acuities/onset. Acute cases require assay times to be readout within 10 min to 2 h for immediate treatment. To realize single EV assays for acute applications is a challenge. Diseases like acute ischemic stroke require timely diagnosis to navigate triage decision schemes, while chronic diseases like cancer, preferably, require same-day results when patients are undergoing treatment

regimens to determine drug responsiveness or resistance to allow for actionable intervention. Ramshani *et al.* presented a simple, rapid, and PCR-free integrated microfluidics system that can quantify both free-floating miRNAs and EV-miRNAs in ~20 μL of sample plasma with 1 pM detection sensitivity in only 30 min, as opposed to a turnaround time of 13 h with 1 mL sample for conventional RT-qPCR.[245]

Cost-Effective and Portable Readout.—Technology that runs single EV assays cannot be expensive, physically bulky, or cumbersome in ways that restrict its usage to centralized laboratory settings. For instance, high resolution equipment like commercial spectrometers are limited to clinical laboratories. To address this, Jahani *et al.* coupled a spectrometer-free optofluidic platform with dielectric metasurfaces to detect BC EVs.[246] Their approach scales down the complex instrumentation to a miniaturized and cost-effective light and camera setup that can reconstruct the spectral shift (to the same effect as seen in commercial spectrometers) induced by femtomolar-level EV interactions on the biosensing interface.

Similarly, the instrumentation required to generate, control, and measure droplets for large scale applications is constrained to laboratory settings. Yelleswarapu *et al.* engineered an optofluidic platform that miniaturizes and parallelizes droplet digital assays into a mobile device readout.[247] By integrating a fluorescent bead processing unit, parallel droplet generators, fluidic delay control, and optical detection, the authors showcase a robust, high-throughput system for low-cost deployment in POC settings.

Multiplexing.—In many instances to distinguish disease specificity, clinical evidence based on a single biomarker is insufficient to determine an appropriate diagnosis of a disease or for treatment monitoring. Therefore, it is highly desirable for a multianalyte screening to profile various analytes simultaneously in single EVs for POC applications. Zhou *et al.* presented a high-throughput and integrated system for rapid single EV analysis of proteins and mRNA/miRNA.[81] Following efficient EV capture from ~90 μL plasma, TIRF microscopy and deep learning were used to quantitatively describe the mRNA, miRNA, and membrane protein cargo with a sample-to-answer time of ~6 h.

Integration.—Conventional EV sample processing requires laborious, multistep sample preparations that require different instruments. To become clinically useful, assays require the ability to integrate modules[248] to realize a “lab-on-a-chip” workflow, reducing the number of steps into a simple, one-step operation. Park *et al.* simplified EV analyses by combining EV sample processing and quantification into a single HiMEX (high-throughput integrated magneto-electrochemical EV) platform.[249] First, Ab-coated magnetic beads are captured and separated target-specific EVs directly from samples without extensive manipulation. Then bead-bound EVs are labeled with probing Abs functionalized with enzyme amplification reactions for electrochemical signal detection. The HiMEX device permitted EV protein profiling directly from clinical samples with a total assay time under 1 h and signals readout in parallel, high-throughput fashion in a 96-well format. As a result, authors were able to conduct diagnostic and longitudinal EV-based studies of colorectal cancer patients during their clinical care.

Clinical Validation: Context of Use.

Clinical validation of single EV techniques requires identifying, measuring, or predicting a meaningful clinical state for a defined context of use. Proof-of-principle studies have effectively indicated their clinical utility for cancer management: (i) early diagnosis, (ii) molecular subtyping/prognostication, and (iii) treatment monitoring, which can also address the management of other diseases.

Early Diagnosis of Disease.—In early work, overexpression of EVs or EV markers was only observed in advanced disease or after detectable tumor progression.[250] Studies predict single EV methods can diagnose cancer at an early stage particularly before metastatic spread, enabling faster treatment decisions and possibly curative surgery.[42] However, there are inherent technical challenges of early biomarker findings that hamper their clinical validation in larger patient cohorts. EV-based methods are emerging to meet these unmet clinical needs. Sun *et al.* designed an integrated EV purification system (EV Click Chips) for minimally invasive and early hepatocellular carcinoma (HCC) detection.[251] Captured EVs (expressing EpCAM, ASGPR1, and CD147) were treated to reverse-transcription ddPCR to obtain a panel of 10 HCC-specific mRNA transcripts. As a result, EV Click Chips enable HCC diagnosis from at-risk cirrhotic patients (~94% sensitive and ~89% specific).

Ferguson *et al.* developed a single EV analysis (sEVA) technique that optimizes SEA[35] for a multiplexed protein analysis (*e.g.*, $KRAS^{mut}$ and $P53^{mut}$) of patient plasma samples to enable early cancer detection.[104] A blinded study validated sEVA could identify vesicles carrying mutant proteins (94% accuracy) with surgically proven stage 1 PDAC. Mathematical models describe the current size LOD of sEVA is estimated to be ~0.1 cm^3 tumor volume, which is below clinical imaging thresholds. Thus, digital EV methods allow for highly sensitive and specific early disease detection (Figure 4D) for symptomatic patients to facilitate faster treatment decisions and EV marker validation for assessing risk in presymptomatic patient populations.

Prognostication: Molecular Subtyping and Disease Staging.—Molecular classification and disease staging are vital to assessing the extent or aggressiveness of disease and selecting prospective treatments. An effort to subtype human BC patients using serum EVs has reported success where EV proteomes cluster based on their molecular subtype (*e.g.*, HER2, TNBC), while the full cellular proteome cannot enable BC subtyping.[12] Thus, developing better EV technologies to validate prognostically relevant EV markers would prove EVs as robust and reliable biomarkers. Work by Reátegui *et al.* described a herringbone microfluidic approach (^{EV}HB-Chip) to isolate tumor EV-RNA from glioblastoma (GBM) patient sera and plasma for downstream RNA-seq analysis and classification into their neural, pro-neural, mesenchymal, and classical subtypes.[101]

Others have been able to establish EV methods to characterize disease progression. Zhang *et al.* developed a nanoengineered chip platform for the multiparametric analysis of EV (EV-CLUE) to analyze matrix metalloprotease 14 expression for *in vitro* cell invasiveness and monitor *in vivo* tumor progression.[252] The authors further demonstrated their device can accurately classify BC patient plasma specimens into 3 groups of distinct BC stages: ductal

carcinoma *in situ*, invasive ductal carcinoma, or metastatic BC from a training cohort (~97% accurate) and a validation cohort (~93% accurate). Thus, EV methods can discriminate different subtypes and stages of a disease (Figure 4D) for stratifying patients into clinical trials and enabling better treatment outcomes.

Treatment Monitoring.—Monitoring the extents of disease burden and therapeutic responses is limited by current imaging or molecular methods. Minimally invasive assays that enable repeatable specimen sampling and an accurate readout of treatment response or disease burden would enable clinicians to adapt therapy accordingly. EV-based methods have been developed to allow real-time monitoring of therapeutic responses.[253,254] Tian *et al.* developed a thermophoretic aptasensor to analyze an EV signature (8 EV protein marker panel) directly from 1 μL of plasma of metastatic BC patients undergoing treatment.[255] The EV signature was profiled longitudinally to monitor treatment responses in training, validation, and prospective cohorts, and served as an independent prognostic factor for progression free survival in metastatic BC patients.

Drugs that target specific molecules may demonstrate promise in preclinical studies, but the emergence of treatment resistance in clinical trials necessitates methods for treatment stratification. EV-based methods are advancing to conduct signaling pathway analysis for how treatments affect a molecular target of interest and its influences in downstream signaling.[256] Shao *et al.* designed an immunomagnetic exosome RNA (iMER) microfluidic chip to assess drug resistance via EV mRNA expression level changes (MGMT and APNG mRNA) from GBM tumor EVs, from Temozolomide initiation to drug resistance.[257] By validating with clinical blood samples from confirmed GBM patients, iMER observed a qualitative match between MGMT and APNG EV mRNA changes and treatment outcomes. It is highly desirable for future clinical use to establish single EV methods to longitudinally monitor treatment responses and probe signal pathways that determine therapeutic efficacy or resistance for optimizing the throughput and accuracy of clinical decision making (Figure 4D).

Case Studies for Central Nervous System Disorders.

Single EV-based liquid biopsy approaches for cancer management can be applied to managing CNS diseases. Diagnosing and monitoring CNS diseases—including acute (stroke, neuro-COVID) and chronic (schizophrenia and major depression) disorders—remain a massive undertaking. Much of our current knowledge of what causes and develops CNS diseases is based on histological studies of post-mortem brain tissue. Unlike tumors, core biopsies of brain tissue are not a viable diagnostic option for evaluating CNS diseases. Probes that allow imaging of the brain have been developed,[258] but more substantial work is required to identify bona fide biomarkers that correlate presence and concentration with disease states. EVs have been observed to cross an intact blood-brain barrier[259,260] and thus can be used for developing tests for CNS disorders with readily accessible sources for sampling such as blood or CSF. It is worth noting that circulating biomarkers are typically low in concentration,[216] such that standard bulk EV methods may not be sensitive enough for detecting rare brain-derived EVs or profiling EV heterogeneity. To tackle this needle-in-

a-haystack challenge, single EV methods that are ultrasensitive and high-throughput are perhaps key to validating reliable CNS disease biomarkers.

Enabling noninvasive readouts of the molecular contents of neuron-derived EVs from CSF or plasma is very exciting, but as the EV field is still in infancy, there are many technical challenges that require troubleshooting. Until recently, researchers have been targeting transmembrane protein L1CAM as an enrichment target to capture neuron-derived EVs as L1CAM is canonically a surface protein expressed on neurons.[261] However, work recently reported by Norman *et al.* confirmed that soluble L1CAM exists in plasma and CSF and is more abundant than EV-expressed L1CAM.[58] Thus, this work signals a re-evaluation of L1CAM as an exclusive neuron-specific EV marker and discover other reliable and reproducible markers to isolate circulating neuron-derived EVs from the human brain.

Acute Neurology: Stroke.—Notably, precipitous conditions like acute ischemic stroke have different etiologies and require early and rapid diagnosis and treatment triage within minutes or hours upon arrival to an emergency department for effective thrombolytic treatment.[262] Consequences of delayed treatment or missing the efficacious therapeutic window results in disability from stroke brain injury, which is a worldwide leading cause of morbidity. EV-based assays have highlighted their potential utility in stroke diagnosis by being able to (i) diagnose transient ischemic attacks[263] and (ii) discriminate ischemic from hemorrhagic stroke subtypes.[264] For example, Wijerathne *et al.* established a microfluidic approach for rapid EV affinity capture and subsequent ddPCR to screen EVs from CD8+ T cells.[265] Analysis of mRNA transcripts (*PLBD1*, *MMP9*, *VCAN*, *FOS*, *CA4*) expressed in CD8+ T cell EVs from AIS patients and controls enabled 80% test positivity for AIS with a turnaround time of 3.7 h. Patients presenting to clinical settings arrive at variable times and are triaged differently. Thus, integrated EV platforms are emerging that deliver results with rapid turnaround times (<60 min), [245,249,266] which could be useful for deciding time-appropriate and POC treatment in acute neurology.

Acute Neurology: Neuro-COVID.—Patients with severe acute respiratory syndrome coronavirus 2 (SARS-CoV-2) infection can develop a range of neurological clinical symptoms and sequalae (neuro-COVID).[267] Although direct infection of the CNS does not seem to be a primary driver of these neurological symptoms,[268] CNS-directed autoantibodies[269] and microvascular dysfunctions[270] likely contribute to the neurological phenotype in COVID-19. Findings have suggested that significant neurodegenerative injury may occur in hospitalized COVID-19 patients and is associated with encephalopathy.[271] Interestingly, blood biomarkers of traumatic brain injury (TBI) are suitable for detecting brain injury in neuro-COVID patients,[272] and by extension, EVs serve as potential sources.

For instance, work by Ko *et al.* described an EV-based assay that maps out a multiplexed panel of EV-miRNA TBI biomarkers from brain-derived GluR2+ EVs following injury, in acute and chronic phases, and combines machine learning to accurately classify various states of brain injury.[273] Similarly, Beard *et al.* combined digital EV techniques to evaluate TBI pathology by profiling EV proteins according to neuronal/glial damage (UCHL1, NFL, Tau, GFAP) and inflammation (IL-6, IL-10, and TNF-α).[274] As a result, profiling the temporal evolution and heterogeneity of EV biomarkers may be applicable

in diagnosing acute manifestations of neuro-COVID and prognosing stages of brain injury/neurodegeneration. Thus, single EV analysis can be leveraged to stratify COVID-19 patients according to neuro-COVID risk for initiating targeted therapies.

Chronic Neuropsychiatric Disorders: Schizophrenia.—Schizophrenia is a complex, heterogeneous mental health disorder characterized by onset of psychosis at adolescence and deteriorating social and cognitive functions.[275] However, it is now well-established that the first psychotic episode is, in fact, a manifestation of advanced disease.[276] There is a time window of months or years prior to the first psychotic break that is characterized by subtle changes in behavioral and cognitive functions—the presyndromal stage. Efforts have been made to alleviate the disorder by intervening at the presyndromal stage to prevent the exacerbation of disease-associated neural impairments. However, staging and predicting schizophrenia trajectories during development has proven difficult due to the lack of validated, sensitive, and specific diagnostic biomarker criteria. Therefore, discovering mechanism-based biomarkers as single EVs would better capture neural circuitry dysfunction to facilitate better patient stratification and monitoring of disease burden and treatment. Most recently, Khadimallah *et al.* determined that by analyzing EVs assumed to be neuronal origin with positive L1CAM expression, combined EV miRNA profiles of miR-137 and COX6A2 as surrogate EV biomarkers of mitochondrial dysfunction in a specific neuron population: parvalbumin interneurons (PVIs).[277] Single EV analysis would be beneficial to dissecting further molecular heterogeneity in PVI-derived EVs to better define disease states in Schizophrenia.

Chronic Neuropsychiatric Disorders: Depression.—Despite strides in treating major depression, one-third of depressed patients remain resistant to antidepressants (ADT).[278] To optimize ADT responses in patients with major depression, a better understanding of treatment response mechanisms is needed. Access to high resolution and high-throughput technologies such as scRNA-seq have facilitated research into the pathophysiology of depression with tissue samples.[279] However, single EV analysis, particularly, can be used to dissect live neuron-specific circuits that are of physiological relevance. Peripheral inflammatory biomarkers have been explored in clinical studies,[280] yet their capacity to reflect brain processes is nonspecific. Instead, probing miRNAs[281,282] packaged into single EVs by resident brain cells provides a window of opportunity to dissect the molecular heterogeneity and subtle changes occurring in mental health disorders and mechanisms of ADT response. This is supported by work from Saeedi *et al.*, where authors determined that altered size and miRNA content is a function of ADT drug response by evaluating L1CAM+ neuron-derived EVs enriched from plasma.[283] Perhaps a single EV analysis can enable a more precise stratification of druggable and unresponsive patient subtypes, which is currently not possible using the Diagnostic and Statistical Manual of Mental Disorders criteria.

CONCLUSIONS

Challenges and Future Outlook.

EV-based liquid biopsies show major clinical promise, but there are important challenges and future developments that need to be addressed before clinical translation.

EVs showcase a complex heterogeneity among their subpopulations with EV size, molecular content, shedding kinetics, universal markers, and cell of origin. Ultrasensitive, high-throughput, and multiplexed technologies are therefore required to profile the different compositions of EV biomarkers at the single EV level. Existing digital methods to analyze individual EVs are in the development pipeline that revolve around Ab–DNA barcoding, ELISA, PCR, flow cytometry, and immunofluorescence imaging. However, single EV analysis is not necessarily a universal solution for biomarker discovery. Bulk approaches like mass spectrometry (for proteins) and sequencing (for nucleic acids) offer unlimited multiplexing capabilities for biomarker exploration that cannot be currently performed using single EV methods. Once biomarkers are discovered, single EV methods can later be used to enrich for different subtypes of EVs.

The translational goal is to capture multiplexed marker measurements in a high-throughput and ultrasensitive manner so that rare, disease-specific EV populations can be identified to their pathological cell-of-origin. To accomplish this, an integrated assay that unifies the entire workflow of—EV enrichment from clinical specimens, signal amplification, signal detection, and signal analysis and interpretation—is required. In this review, we have outlined the emerging developments and challenges for each design aspect of the entire assay pipeline. First, variabilities in EV purification are due to contamination by lipid and protein particles that share similar physical characteristics, as well as poor multiplexing due to limited availability of affinity capture probes and variable binding affinities. Second, signal amplification is mostly dependent on enzyme-based fluorescence or nucleic acid amplification, and multispectral materials that exist as microscale beads need to be size matched with EVs at the nanoscale. Third, signal detection can involve challenges such as limited single-base detection and fast translocation times for nanopore sequencing or using state-of-the-art nanofabrication techniques to preserve optical resonance parameters for nanoplasmonics. Fourth, performing a parallel proteomic and transcriptomic analysis of single EVs can be difficult as nucleic acid species are scarce in single EVs and lack capture sequences present in single cells. Furthermore, machine learning algorithms can be susceptible to data overfitting. An overwhelming challenge, however, is the integration of all these assay modules into a complete “lab-on-a-chip” workflow, while leveraging high sensitivity, high-throughput, and multiplexing capacities.

Advancing digital EV assays for clinical applications relies on interdisciplinary collaborations among technology developers and end users (biologists and clinicians). Also, convincing stakeholders to adopt digital EV methods into the clinic requires commercialized and integrated assays that meet the criteria of rapid turnaround times, cost-effectiveness and portability, and multiplexing. In addition, the standardization of preanalytical steps (sample preparation and purification), quantification, and methods reporting is important to ensure robust and reproducible assay performance among the user community. At the moment,

EV methods are being clinically validated for different contexts of use, ranging from early disease diagnosis, prognostication, and treatment monitoring. While single EV assays are making strides in cancer management, we envision potential utility for also managing various acute and chronic diseases. By satisfying these critical needs, a more in-depth and precise dissection of EV heterogeneity will help accelerate biomarker characterization for disease monitoring and management.

ACKNOWLEDGMENTS

The authors are grateful to David E. Reynolds, George C. Galanis, and Kevin Guan for many helpful discussions. Figures were created with Biorender.com.

Funding

This work was supported by NIH NCI K99/R00 (K99CA256353).

REFERENCES

(1). Kalluri R; LeBleu VS The biology, function, and biomedical applications of exosomes. Science. 2020, 367, eaau6977. [PubMed: 32029601]

(2). Yáñez-Mó M; Siljander PRM; Andreu Z; Bedina Zavec A; Borraàs FE; Buzas EI; Buzas K; Casal E; Cappello F; Carvalho J; Colás E; Cordeiro-da Silva A; Fais S; Falcon-Perez JM; Ghobrial IM; Giebel B; Gimona M; Graner M; Gursel I; Gursel M; et al. Biological properties of extracellular vesicles and their physiological functions. J. Extracell. Vesicles 2015, 4, 27066. [PubMed: 25979354]

(3). van Niel G; D'Angelo G; Raposo G Shedding light on the cell biology of extracellular vesicles. Nat. Rev. Mol. Cell Biol 2018, 19, 213–228. [PubMed: 29339798]

(4). Shah R; Patel T; Freedman JE Circulating Extracellular Vesicles in Human Disease. N. Engl. J. Med 2018, 379, 958–966. [PubMed: 30184457]

(5). Ullal Adeeti V; Peterson V; Agasti Sarit S; Tuang S; Juric D; Castro Cesar M; Weissleder R Cancer Cell Profiling by Barcoding Allows Multiplexed Protein Analysis in Fine-Needle Aspirates. Sci. Transl. Med 2014, 6, 219ra219.

(6). Cheng L; Sharples RA; Scicluna BJ; Hill AF Exosomes provide a protective and enriched source of miRNA for biomarker profiling compared to intracellular and cell-free blood. J. Extracell. Vesicles 2014, 3, 23743.

(7). Wu M; Ouyang Y; Wang Z; Zhang R; Huang P-H; Chen C; Li H; Li P; Quinn D; Dao M; Suresh S; Sadovsky Y; Huang TJ Isolation of exosomes from whole blood by integrating acoustics and microfluidics. Proc. Natl. Acad. Sci. U. S. A 2017, 114, 10584–10589. [PubMed: 28923936]

(8). Wu C-X; Liu Z-F Proteomic Profiling of Sweat Exosome Suggests its Involvement in Skin Immunity. J. Invest. Dermatol 2018, 138, 89–97. [PubMed: 28899687]

(9). Pisitkun T; Shen R-F; Knepper MA Identification and proteomic profiling of exosomes in human urine. Proc. Natl. Acad. Sci. U.S.A 2004, 101, 13368–13373. [PubMed: 15326289]

(10). Street JM; Barran PE; Mackay CL; Weidt S; Balmforth C; Walsh TS; Chalmers RTA; Webb DJ; Dear JW Identification and proteomic profiling of exosomes in human cerebrospinal fluid. J. Transl. Med 2012, 10, 5. [PubMed: 22221959]

(11). Palanisamy V; Sharma S; Deshpande A; Zhou H; Gimzewski J; Wong DT Nanostructural and Transcriptomic Analyses of Human Saliva Derived Exosomes. PLoS One. 2010, 5, e8577. [PubMed: 20052414]

(12). Rontogianni S; Synadaki E; Li B; Liefaard MC; Lips EH; Wesseling J; Wu W; Altelaar M Proteomic profiling of extracellular vesicles allows for human breast cancer subtyping. Commun. Biol 2019, 2, 325. [PubMed: 31508500]

(13). Kugeratski FG; Hodge K; Lilla S; McAndrews KM; Zhou X; Hwang RF; Zanivan S; Kalluri R Quantitative proteomics identifies the core proteome of exosomes with syntenin-1 as the highest

abundant protein and a putative universal biomarker. Nat. Cell Biol 2021, 23, 631–641. [PubMed: 34108659]

(14). Valadi H; Ekström K; Bossios A; Sjöstrand M; Lee JJ; Lötvall JO Exosome-mediated transfer of mRNAs and microRNAs is a novel mechanism of genetic exchange between cells. Nat. Cell Biol 2007, 9, 654–659. [PubMed: 17486113]

(15). Mittelbrunn M; Gutiérrez-Vázquez C; Villarroya-Beltri C; González S; Sánchez-Cabo F; González MÁ; Bernad A; Sánchez-Madrid F Unidirectional transfer of microRNA-loaded exosomes from T cells to antigen-presenting cells. Nat. Commun 2011, 2, 282. [PubMed: 21505438]

(16). Balaj L; Lessard R; Dai L; Cho Y-J; Pomeroy SL; Breakefield XO; Skog J Tumour microvesicles contain retrotransposon elements and amplified oncogene sequences. Nat. Commun 2011, 2, 180. [PubMed: 21285958]

(17). Skog J; Wuürdinger T; van Rijn S; Meijer DH; Gainche L; Curry WT; Carter BS; Krichevsky AM; Breakefield XO Glioblastoma microvesicles transport RNA and proteins that promote tumour growth and provide diagnostic biomarkers. Nat. Cell Biol 2008, 10, 1470–1476. [PubMed: 19011622]

(18). Allenson K; Castillo J; San Lucas FA; Scelo G; Kim DU; Bernard V; Davis G; Kumar T; Katz M; Overman MJ; Foretova L; Fabianova E; Holcatova I; Janout V; Meric-Bernstam F; Gascoyne P; Wistuba I; Varadhachary G; Brennan P; Hanash S; et al. High prevalence of mutant *KRAS* in circulating exosome-derived DNA from early-stage pancreatic cancer patients. Ann. Oncol 2017, 28, 741–747. [PubMed: 28104621]

(19). Wan Y; Liu B; Lei H; Zhang B; Wang Y; Huang H; Chen S; Feng Y; Zhu L; Gu Y; Zhang Q; Ma H; Zheng SY Nanoscale extracellular vesicle-derived DNA is superior to circulating cell-free DNA for mutation detection in early-stage non-small-cell lung cancer. Ann. Oncol 2018, 29, 2379–2383. [PubMed: 30339193]

(20). Théry C; Ostrowski M; Segura E Membrane vesicles as conveyors of immune responses. Nat. Rev. Immunol 2009, 9, 581–593. [PubMed: 19498381]

(21). Nolte-'t Hoen E; Cremer T; Gallo RC; Margolis LB Extracellular vesicles and viruses: Are they close relatives? Proc. Natl. Acad. Sci. U. S. A 2016, 113, 9155–9161. [PubMed: 27432966]

(22). Sahoo S; Adamiak M; Mathiyalagan P; Kenneweg F; Kafert-Kasting S; Thum T Therapeutic and Diagnostic Translation of Extracellular Vesicles in Cardiovascular Diseases. Circulation. 2021, 143, 1426–1449. [PubMed: 33819075]

(23). Budnik V; Ruiz-Canñada C; Wendler F Extracellular vesicles round off communication in the nervous system. Nat. Rev. Neurosci 2016, 17, 160–172. [PubMed: 26891626]

(24). Al-Nedawi K; Meehan B; Micallef J; Lhotak V; May L; Guha A; Rak J Intercellular transfer of the oncogenic receptor EGFRvIII by microvesicles derived from tumour cells. Nat. Cell Biol 2008, 10, 619–624. [PubMed: 18425114]

(25). Hoshino A; Costa-Silva B; Shen T-L; Rodrigues G; Hashimoto A; Tesic Mark M; Molina H; Kohsaka S; Di Giannatale A; Ceder S; Singh S; Williams C; Soplop N; Uryu K; Pharmer L; King T; Bojmar L; Davies AE; Ararso Y; Zhang T; et al. Tumour exosome integrins determine organotropic metastasis. Nature. 2015, 527, 329–335. [PubMed: 26524530]

(26). Ullah M; Kodam SP; Mu Q; Akbar A Microbubbles versus Extracellular Vesicles as Therapeutic Cargo for Targeting Drug Delivery. ACS Nano 2021, 15, 3612–3620. [PubMed: 33666429]

(27). Xia Y; Hu G; Chen Y; Yuan J; Zhang J; Wang S; Li Q; Wang Y; Deng Z Embryonic Stem Cell Derived Small Extracellular Vesicles Modulate Regulatory T Cells to Protect against Ischemic Stroke. ACS Nano 2021, 15, 7370–7385. [PubMed: 33733738]

(28). Ko K-W; Park S-Y; Lee EH; Yoo Y-I; Kim D-S; Kim JY; Kwon TG; Han DK Integrated Bioactive Scaffold with Polydeoxyribonucleotide and Stem-Cell-Derived Extracellular Vesicles for Kidney Regeneration. ACS Nano 2021, 15, 7575–7585. [PubMed: 33724774]

(29). Wang J; Wang C; Cai P; Luo Y; Cui Z; Loh XJ; Chen X Artificial Sense Technology: Emulating and Extending Biological Senses. ACS Nano 2021, 15, 18671–18678. [PubMed: 34881877]

(30). Coumans FAW; Brisson AR; Buzas EI; Dignat-George F; Drees EEE; El-Andaloussi S; Emanueli C; Gasecka A; Hendrix A; Hill AF; Lacroix R; Lee Y; van Leeuwen TG; Mackman N; Mäger I;

Nolan JP; van der Pol E; Pegtel DM; Sahoo S; Siljander PRM; et al. Methodological Guidelines to Study Extracellular Vesicles. Circ. Res 2017, 120, 1632–1648. [PubMed: 28495994]

(31). Bordanaba-Florit G; Royo F; Kruglik SG; Falcón-Pérez JM Using single-vesicle technologies to unravel the heterogeneity of extracellular vesicles. Nat. Protoc 2021, 16, 3163–3185. [PubMed: 34135505]

(32). You Y; Muraoka S; Jedrychowski MP; Hu J; McQuade AK; Young-Pearse T; Aslebagh R; Shaffer SA; Gygi SP; Blurton-Jones M; Poon WW; Ikezu T Human neural cell type-specific extracellular vesicle proteome defines disease-related molecules associated with activated astrocytes in Alzheimer's disease brain. J. Extracell. Vesicles 2022, 11, e12183. [PubMed: 35029059]

(33). Kowal J; Arras G; Colombo M; Jouve M; Morath JP; Primdal-Bengtson B; Dingli F; Loew D; Tkach M; Théry C Proteomic comparison defines novel markers to characterize heterogeneous populations of extracellular vesicle subtypes. Proc. Natl. Acad. Sci. U. S. A 2016, 113, E968–E977. [PubMed: 26858453]

(34). Nikoloff JM; Saucedo-Espinosa MA; Kling A; Dittrich PS Identifying extracellular vesicle populations from single cells. Proc. Natl. Acad. Sci. U. S. A 2021, 118, e2106630118. [PubMed: 34518226]

(35). Lee K; Fraser K; Ghaddar B; Yang K; Kim E; Balaj L; Chiocca EA; Breakefield XO; Lee H; Weissleder R Multiplexed Profiling of Single Extracellular Vesicles. ACS Nano 2018, 12, 494–503. [PubMed: 29286635]

(36). Fraser K; Jo A; Giedt J; Vinegoni C; Yang KS; Peruzzi P; Chiocca EA; Breakefield XO; Lee H; Weissleder R Characterization of single microvesicles in plasma from glioblastoma patients. Neuro-Oncology 2019, 21, 606–615. [PubMed: 30561734]

(37). Raposo G; Stoorvogel W Extracellular vesicles: Exosomes, microvesicles, and friends. J. Cell Biol 2013, 200, 373–383. [PubMed: 23420871]

(38). Burbidge K; Zwikelmaier V; Cook B; Long MM; Balva B; Lonigro M; Ispas G; Rademacher DJ; Campbell EM Cargo and cell-specific differences in extracellular vesicle populations identified by multiplexed immunofluorescent analysis. J. Extracell. Vesicles 2020, 9, 1789326. [PubMed: 32944176]

(39). Zhang H; Freitas D; Kim HS; Fabijanic K; Li Z; Chen H; Mark MT; Molina H; Martin AB; Bojmar L; Fang J; Rampersaud S; Hoshino A; Matei I; Kenific CM; Nakajima M; Mutvei AP; Sansone P; Buehring W; Wang H; et al. Identification of distinct nanoparticles and subsets of extracellular vesicles by asymmetric flow field-flow fractionation. Nat. Cell Biol 2018, 20, 332–343. [PubMed: 29459780]

(40). Di Vizio D; Kim J; Hager MH; Morello M; Yang W; Lafargue CJ; True LD; Rubin MA; Adam RM; Beroukhim R; Demichelis F; Freeman MR Oncosome Formation in Prostate Cancer: Association with a Region of Frequent Chromosomal Deletion in Metastatic Disease. Cancer Res. 2009, 69, 5601–5609. [PubMed: 19549916]

(41). Zijlstra A; Di Vizio D Size matters in nanoscale communication. Nat. Cell Biol 2018, 20, 228–230. [PubMed: 29476154]

(42). Ferguson S; Weissleder R Modeling EV Kinetics for Use in Early Cancer Detection. Adv. Biosyst 2020, 4, 1900305.

(43). Kreimer S; Belov AM; Ghiran I; Murthy SK; Frank DA; Ivanov AR Mass-Spectrometry-Based Molecular Characterization of Extracellular Vesicles: Lipidomics and Proteomics. J. Proteome Res 2015, 14, 2367–2384. [PubMed: 25927954]

(44). van der Pol E; Coumans FAW; Grootemaat AE; Gardiner C; Sargent IL; Harrison P; Sturk A; van Leeuwen TG; Nieuwland R Particle size distribution of exosomes and microvesicles determined by transmission electron microscopy, flow cytometry, nanoparticle tracking analysis, and resistive pulse sensing. J. Thromb. Haemostasis 2014, 12, 1182–1192. [PubMed: 24818656]

(45). O'Brien K; Breyne K; Ughetto S; Laurent LC; Breakefield XO RNA delivery by extracellular vesicles in mammalian cells and its applications. Nat. Rev. Mol. Cell Biol 2020, 21, 585–606. [PubMed: 32457507]

(46). Todkar K; Chikhi L; Desjardins V; El-Mortada F; Pépin G; Germain M Selective packaging of mitochondrial proteins into extracellular vesicles prevents the release of mitochondrial DAMPs. Nat. Commun 2021, 12, 1971. [PubMed: 33785738]

(47). Wei Z; Batagov AO; Schinelli S; Wang J; Wang Y; El Fatimy R; Rabinovsky R; Balaj L; Chen CC; Hochberg F; Carter B; Breakefield XO; Krichevsky AM Coding and noncoding landscape of extracellular RNA released by human glioma stem cells. Nat. Commun 2017, 8, 1145. [PubMed: 29074968]

(48). Chevillet JR; Kang Q; Ruf IK; Briggs HA; Vojtech LN; Hughes SM; Cheng HH; Arroyo JD; Meredith EK; Gallichotte EN; Pogosova-Agadjanyan EL; Morrissey C; Stirewalt DL; Hladik F; Yu EY; Higano CS; Tewari M Quantitative and stoichiometric analysis of the microRNA content of exosomes. Proc. Natl. Acad. Sci. U. S. A 2014, 111, 14888–14893. [PubMed: 25267620]

(49). Rissin DM; Kan CW; Campbell TG; Howes SC; Fournier DR; Song L; Piech T; Patel PP; Chang L; Rivnak AJ; Ferrell EP; Randall JD; Provuncher GK; Walt DR; Duffy DC Single-molecule enzyme-linked immunosorbent assay detects serum proteins at subfemtomolar concentrations. Nat. Biotechnol 2010, 28, 595–599. [PubMed: 20495550]

(50). Basu AS Digital Assays Part I: Partitioning Statistics and Digital PCR. SLAS Technology Translating Life Sciences Innovation 2017, 22, 369–386.

(51). Ven K; Vanspauwen B; Pérez-Ruiz E; Leirs K; Decrop D; Gerstmans H; Spasic D; Lammertyn J Target Confinement in Small Reaction Volumes Using Microfluidic Technologies: A Smart Approach for Single-Entity Detection and Analysis. ACS Sens. 2018, 3, 264–284. [PubMed: 29363316]

(52). Ayers L; Pink R; Carter DRF; Nieuwland R Clinical requirements for extracellular vesicle assays. J. Extracell. Vesicles 2019, 8, 1593755. [PubMed: 30949310]

(53). Klein AM; Mazutis L; Akartuna I; Tallapragada N; Veres A; Li V; Peshkin L; Weitz DA; Kirschner MW Droplet Barcoding for Single-Cell Transcriptomics Applied to Embryonic Stem Cells. Cell. 2015, 161, 1187–1201. [PubMed: 26000487]

(54). Tian Q; He C; Liu G; Zhao Y; Hui L; Mu Y; Tang R; Luo Y; Zheng S; Wang B Nanoparticle Counting by Microscopic Digital Detection: Selective Quantitative Analysis of Exosomes via Surface-Anchored Nucleic Acid Amplification. Anal. Chem 2018, 90, 6556–6562. [PubMed: 29715009]

(55). Ko J; Wang Y; Sheng K; Weitz DA; Weissleder R Sequencing-Based Protein Analysis of Single Extracellular Vesicles. ACS Nano 2021, 15, 5631–5638. [PubMed: 33687214]

(56). Ko J; Wang Y; Carlson JCT; Marquard A; Gungabeesoon J; Charest A; Weitz D; Pittet MJ; Weissleder R Single Extracellular Vesicle Protein Analysis Using Immuno-Droplet Digital Polymerase Chain Reaction Amplification. Adv. Biosyst 2020, 4, 1900307.

(57). Wu D; Yan J; Shen X; Sun Y; Thulin M; Cai Y; Wik L; Shen Q; Oelrich J; Qian X; Dubois KL; Ronquist KG; Nilsson M; Landegren U; Kamali-Moghaddam M Profiling surface proteins on individual exosomes using a proximity barcoding assay. Nat. Commun 2019, 10, 3854. [PubMed: 31451692]

(58). Norman M; Ter-Ovanesyan D; Trieu W; Lazarovits R; Kowal EJK; Lee JH; Chen-Plotkin AS; Regev A; Church GM; Walt DR L1CAM is not associated with extracellular vesicles in human cerebrospinal fluid or plasma. Nat. Methods 2021, 18, 631–634. [PubMed: 34092791]

(59). Ter-Ovanesyan D; Norman M; Lazarovits R; Trieu W; Lee J-H; Church GM; Walt DR Framework for rapid comparison of extracellular vesicle isolation methods. eLife. 2021, 10, e70725. [PubMed: 34783650]

(60). Wei P; Wu F; Kang B; Sun X; Heskia F; Pachot A; Liang J; Li D Plasma extracellular vesicles detected by Single Molecule array technology as a liquid biopsy for colorectal cancer. J. Extracell. Vesicles 2020, 9, 1809765. [PubMed: 32944195]

(61). Shim J.-u.; Ranasinghe RT; Smith CA; Ibrahim SM; Hollfelder F; Huck WTS; Klenerman D; Abell C Ultrarapid Generation of Femtoliter Microfluidic Droplets for Single-Molecule-Counting Immunoassays. ACS Nano 2013, 7, 5955–5964. [PubMed: 23805985]

(62). Liu C; Xu X; Li B; Situ B; Pan W; Hu Y; An T; Yao S; Zheng L Single-Exosome-Counting Immunoassays for Cancer Diagnostics. Nano Lett. 2018, 18, 4226–4232. [PubMed: 29888919]

(63). Yang Z; Atiyas Y; Shen H; Siedlik MJ; Wu J; Beard K; Fonar G; Dolle JP; Smith DH; Eberwine JH; Meaney DF; Issadore DA Ultrasensitive Single Extracellular Vesicle Detection Using High Throughput Droplet Digital Enzyme-Linked Immunosorbent Assay. Nano Lett. 2022, 22, 4315. [PubMed: 35588529]

(64). Vogelstein B; Kinzler KW Digital PCR. Proc. Natl. Acad. Sci. U. S. A 1999, 96, 9236–9241. [PubMed: 10430926]

(65). Morley AA Digital PCR: A brief history. Biomol. Detect. Quantif 2014, 1, 1–2. [PubMed: 27920991]

(66). Hindson BJ; Ness KD; Masquelier DA; Belgrader P; Heredia NJ; Makarewicz AJ; Bright IJ; Lucero MY; Hiddessen AL; Legler TC; Kitano TK; Hodel MR; Petersen JF; Wyatt PW; Steenblock ER; Shah PH; Bousse LJ; Troup CB; Mellen JC; Wittmann DK; et al. High-Throughput Droplet Digital PCR System for Absolute Quantitation of DNA Copy Number. Anal. Chem 2011, 83, 8604–8610. [PubMed: 22035192]

(67). Hindson CM; Chevillet JR; Briggs HA; Gallichotte EN; Ruf IK; Hindson BJ; Vessella RL; Tewari M Absolute quantification by droplet digital PCR versus analog real-time PCR. Nat. Methods 2013, 10, 1003–1005. [PubMed: 23995387]

(68). Diehl F; Li M; He Y; Kinzler KW; Vogelstein B; Dressman D BEAMing: single-molecule PCR on microparticles in water-in-oil emulsions. Nat. Methods 2006, 3, 551–559. [PubMed: 16791214]

(69). Chen WW; Balaj L; Liau LM; Samuels ML; Kotsopoulos SK; Maguire CA; LoGuidice L; Soto H; Garrett M; Zhu LD; Sivaraman S; Chen C; Wong ET; Carter BS; Hochberg FH; Breakefield XO; Skog J BEAMing and Droplet Digital PCR Analysis of Mutant IDH1 mRNA in Glioma Patient Serum and Cerebrospinal Fluid Extracellular Vesicles. Molecular Therapy - Nucleic Acids. 2013, 2, e109. [PubMed: 23881452]

(70). Lin B; Tian T; Lu Y; Liu D; Huang M; Zhu L; Zhu Z; Song Y; Yang C Tracing Tumor-Derived Exosomal PD-L1 by Dual-Aptamer Activated Proximity-Induced Droplet Digital PCR. Angew. Chem., Int. Ed 2021, 60, 7582–7586.

(71). Welsh JA; Killingsworth B; Kepley J; Traynor T; Cook S; Savage J; Marte J; Lee M-J; Maeng HM; Pleet ML; Magana S; Gorgens A; Maire CL; Lamszus K; Ricklefs FL; Merino MJ; Linehan WM; Greten T; Cooks T; Harris CC; et al. MPAPASS software enables stitched multiplex, multidimensional EV repertoire analysis and a standard framework for reporting bead-based assays. Cells Rep. Methods 2022, 2, 100136.

(72). Van Der Pol E; Van Gemert MJC; Sturk A; Nieuwland R; Van Leeuwen TG Single vs. swarm detection of microparticles and exosomes by flow cytometry. J. Thromb. Haemostasis 2012, 10, 919–930. [PubMed: 22394434]

(73). Yang KS; Lin H-Y; Curley C; Welch MW; Wolpin BM; Lee H; Weissleder R; Im H; Castro CM Bead-Based Extracellular Vesicle Analysis Using Flow Cytometry. Adv. Biosyst 2020, 4, 2000203.

(74). Görgens A; Bremer M; Ferrer-Tur R; Murke F; Tertel T; Horn PA; Thalmann S; Welsh JA; Probst C; Guerin C; Boulanger CM; Jones JC; Hanenberg H; Erdbrügger U; Lannigan J; Ricklefs FL; El-Andaloussi S; Giebel B Optimisation of imaging flow cytometry for the analysis of single extracellular vesicles by using fluorescence-tagged vesicles as biological reference material. J. Extracell. Vesicles 2019, 8, 1587567. [PubMed: 30949308]

(75). Löf L; Ebai T; Dubois L; Wik L; Ronquist KG; Nolander O; Lundin E; Söderberg O; Landegren U; Kamali-Moghaddam M Detecting individual extracellular vesicles using a multicolor in situ proximity ligation assay with flow cytometric readout. Sci. Rep 2016, 6, 34358. [PubMed: 27681459]

(76). Shen W; Guo K; Adkins GB; Jiang Q; Liu Y; Sedano S; Duan Y; Yan W; Wang SE; Bergersen K; Worth D; Wilson EH; Zhong W A Single Extracellular Vesicle (EV) Flow Cytometry Approach to Reveal EV Heterogeneity. Angew. Chem., Int. Ed 2018, 57, 15675–15680.

(77). Dong L; Zieren RC; Horie K; Kim C-J; Mallick E; Jing Y; Feng M; Kuczler MD; Green J; Amend SR; Witwer KW; de Reijke TM; Cho Y-K; Pienta KJ; Xue W Comprehensive evaluation of methods for small extracellular vesicles separation from human plasma, urine and cell culture medium. J. Extracell. Vesicles. 2020, 10, e12044. [PubMed: 33489012]

(78). Tian Y; Ma L; Gong M; Su G; Zhu S; Zhang W; Wang S; Li Z; Chen C; Li L; Wu L; Yan X Protein Profiling and Sizing of Extracellular Vesicles from Colorectal Cancer Patients via Flow Cytometry. ACS Nano 2018, 12, 671–680. [PubMed: 29300458]

(79). Panagopoulou MS; Wark AW; Birch DJS; Gregory CD Phenotypic analysis of extracellular vesicles: a review on the applications of fluorescence. J. Extracell. Vesicles 2020, 9, 1710020. [PubMed: 32002172]

(80). He D; Wang H; Ho S-L; Chan H-N; Hai L; He X; Wang K; Li H-W Total internal reflection-based single-vesicle in situ quantitative and stoichiometric analysis of tumor-derived exosomal microRNAs for diagnosis and treatment monitoring. Theranostics. 2019, 9, 4494–4507. [PubMed: 31285775]

(81). Zhou J; Wu Z; Hu J; Yang D; Chen X; Wang Q; Liu J; Dou M; Peng W; Wu Y; Wang W; Xie C; Wang M; Song Y; Zeng H; Bai C High-throughput single-EV liquid biopsy: Rapid, simultaneous, and multiplexed detection of nucleic acids, proteins, and their combinations. Sci. Adv 2020, 6, eabc1204. [PubMed: 33219024]

(82). Cho S; Yi J; Kwon Y; Kang H; Han C; Park J Multifluorescence Single Extracellular Vesicle Analysis by Time-Sequential Illumination and Tracking. ACS Nano 2021, 15, 11753–11761. [PubMed: 34181396]

(83). Akama K; Shirai K; Suzuki S Droplet-Free Digital Enzyme-Linked Immunosorbent Assay Based on a Tyramide Signal Amplification System. Anal. Chem 2016, 88, 7123–7129. [PubMed: 27322525]

(84). Akama K; Iwanaga N; Yamawaki K; Okuda M; Jain K; Ueno H; Soga N; Minagawa Y; Noji H Wash- and Amplification-Free Digital Immunoassay Based on Single-Particle Motion Analysis. ACS Nano 2019, 13, 13116–13126. [PubMed: 31675215]

(85). Wu C; Garden PM; Walt DR Ultrasensitive Detection of Attomolar Protein Concentrations by Dropcast Single Molecule Assays. J. Am. Chem. Soc 2020, 142, 12314–12323. [PubMed: 32602703]

(86). Wu C; Dougan TJ; Walt DR High-Throughput, High-Multiplex Digital Protein Detection with Attomolar Sensitivity. ACS Nano 2022, 16, 1025–1035. [PubMed: 35029381]

(87). Ko J; Bhagwat N; Yee SS; Black T; Redlinger C; Romeo J; O'Hara M; Raj A; Carpenter EL; Stanger BZ; Issadore D A magnetic micropore chip for rapid (<1 h) unbiased circulating tumor cell isolation and in situ RNA analysis. Lab Chip. 2017, 17, 3086–3096. [PubMed: 28809985]

(88). Wang Z; Ahmed S; Labib M; Wang H; Hu X; Wei J; Yao Y; Moffat J; Sargent EH; Kelley SO Efficient recovery of potent tumour-infiltrating lymphocytes through quantitative immunomagnetic cell sorting. Nat. Biomed. Eng 2022, 6, 108–117. [PubMed: 35087171]

(89). Li P; Mao Z; Peng Z; Zhou L; Chen Y; Huang P-H; Truica CI; Drabick JJ; El-Deiry WS; Dao M; Suresh S; Huang TJ Acoustic separation of circulating tumor cells. Proc. Natl. Acad. Sci. U. S. A 2015, 112, 4970–4975. [PubMed: 25848039]

(90). Augustsson P; Karlsen JT; Su H-W; Bruus H; Voldman J Iso-acoustic focusing of cells for size-insensitive acousto-mechanical phenotyping. Nat. Commun 2016, 7, 11556. [PubMed: 27180912]

(91). Faraghat SA; Hoettges KF; Steinbach MK; van der Veen DR; Brackenbury WJ; Henslee EA; Labeed FH; Hughes MP High-throughput, low-loss, low-cost, and label-free cell separation using electrophysiology-activated cell enrichment. Proc. Natl. Acad. Sci. U. S. A 2017, 114, 4591–4596. [PubMed: 28408395]

(92). Menze L; Duarte PA; Haddon L; Chu M; Chen J Selective Single-Cell Sorting Using a Multisectorial Electroactive Nanowell Platform. ACS Nano 2022, 16, 211–220. [PubMed: 34559518]

(93). Lee K; Shao H; Weissleder R; Lee H Acoustic Purification of Extracellular Microvesicles. ACS Nano 2015, 9, 2321–2327. [PubMed: 25672598]

(94). Jeong S; Park J; Pathania D; Castro CM; Weissleder R; Lee H Integrated Magneto–Electrochemical Sensor for Exosome Analysis. ACS Nano 2016, 10, 1802–1809. [PubMed: 26808216]

(95). Van Deun J; Mestdagh P; Sormunen R; Cocquyt V; Vermaelen K; Vandesompele J; Bracke M; De Wever O; Hendrix A The impact of disparate isolation methods for extracellular vesicles on downstream RNA profiling. J. Extracell. Vesicles 2014, 3, 24858.

(96). Linares R; Tan S; Gounou C; Arraud N; Brisson AR High-speed centrifugation induces aggregation of extracellular vesicles. J. Extracell. Vesicles 2015, 4, 29509. [PubMed: 26700615]

(97). Liga A; Vliegenthart ADB; Oosthuyzen W; Dear JW; Kersaudy-Kerhoas M Exosome isolation: a microfluidic road-map. Lab Chip. 2015, 15, 2388–2394. [PubMed: 25940789]

(98). Wan Y; Cheng G; Liu X; Hao S-J; Nisic M; Zhu C-D; Xia Y-Q; Li W-Q; Wang Z-G; Zhang W-L; Rice SJ; Sebastian A; Albert I; Belani CP; Zheng S-Y Rapid magnetic isolation of extracellular vesicles via lipid-based nanoprobes. Nat. Biomed. Eng 2017, 1, 0058. [PubMed: 28966872]

(99). Lobb RJ; Becker M; Wen Wen S; Wong CSF; Wiegmans AP; Leimgruber A; Möller A Optimized exosome isolation protocol for cell culture supernatant and human plasma. J. Extracell. Vesicles 2015, 4, 27031. [PubMed: 26194179]

(100). Squires TM; Messinger RJ; Manalis SR Making it stick: convection, reaction and diffusion in surface-based biosensors. Nat. Biotechnol 2008, 26, 417–426. [PubMed: 18392027]

(101). Reátegui E; van der Vos KE; Lai CP; Zeinali M; Atai NA; Aldikacti B; Floyd FP; H. Khankhel A; Thapar V; Hochberg FH; Sequist LV; Nahed BV; S. Carter B; Toner M; Balaj L; T. Ting D; Breakefield XO; Stott SL Engineered nanointerfaces for microfluidic isolation and molecular profiling of tumor-specific extracellular vesicles. Nat. Commun 2018, 9, 175. [PubMed: 29330365]

(102). Zhang P; Zhou X; He M; Shang Y; Tetlow AL; Godwin AK; Zeng Y Ultrasensitive detection of circulating exosomes with a 3D-nanopatterned microfluidic chip. Nat. Biomed. Eng 2019, 3, 438–451. [PubMed: 31123323]

(103). Yang KS; Im H; Hong S; Pergolini I; del Castillo AF; Wang R; Clardy S; Huang C-H; Pille C; Ferrone S; Yang R; Castro CM; Lee H; del Castillo CF; Weissleder R Multiparametric plasma EV profiling facilitates diagnosis of pancreatic malignancy. Sci. Transl. Med 2017, 9, eaa13226.

(104). Ferguson S; Yang KS; Zelga P; Liss AS; Carlson JCT; del Castillo CF; Weissleder R Single-EV analysis (sEVA) of mutated proteins allows detection of stage 1 pancreatic cancer. Sci. Adv 2022, 8, eabm3453. [PubMed: 35452280]

(105). Juncker D; Bergeron S; Laforte V; Li H Cross-reactivity in antibody microarrays and multiplexed sandwich assays: shedding light on the dark side of multiplexing. Curr. Opin. Chem. Biol 2014, 18, 29–37. [PubMed: 24534750]

(106). Ellington AA; Kullo IJ; Bailey KR; Klee GG Antibody-Based Protein Multiplex Platforms: Technical and Operational Challenges. Clin. Chem 2010, 56, 186–193. [PubMed: 19959625]

(107). Dunn MR; Jimenez RM; Chaput JC Analysis of aptamer discovery and technology. Nat. Rev. Chem 2017, 1, 0076.

(108). Liu C; Zhao J; Tian F; Chang J; Zhang W; Sun J λ-DNA- and Aptamer-Mediated Sorting and Analysis of Extracellular Vesicles. J. Am. Chem. Soc 2019, 141, 3817–3821. [PubMed: 30789261]

(109). He D; Ho S-L; Chan H-N; Wang H; Hai L; He X; Wang K; Li H-W Molecular-Recognition-Based DNA Nanodevices for Enhancing the Direct Visualization and Quantification of Single Vesicles of Tumor Exosomes in Plasma Microsamples. Anal. Chem 2019, 91, 2768–2775. [PubMed: 30644724]

(110). Kacherovsky N; Cardle II; Cheng EL; Yu JL; Baldwin ML; Salipante SJ; Jensen MC; Pun SH Traceless aptamer-mediated isolation of CD8+ T cells for chimeric antigen receptor T-cell therapy. Nat. Biomed. Eng 2019, 3, 783–795. [PubMed: 31209354]

(111). Gray BP; Requena MD; Nichols MD; Sullenger BA Aptamers as Reversible Sorting Ligands for Preparation of Cells in Their Native State. Cell Chem. Biol 2020, 27, 232. [PubMed: 31879266]

(112). Wu D; Gordon CKL; Shin JH; Eisenstein M; Soh HT Directed Evolution of Aptamer Discovery Technologies. Acc. Chem. Res 2022, 55, 685–695. [PubMed: 35130439]

(113). Yoshikawa AM; Wan L; Zheng L; Eisenstein M; Soh HT A system for multiplexed selection of aptamers with exquisite specificity without counterselection. Proc. Natl. Acad. Sci. U. S. A 2022, 119, e2119945119. [PubMed: 35290115]

(114). Townshend B; Xiang JS; Manzanarez G; Hayden EJ; Smolke CD A multiplexed, automated evolution pipeline enables scalable discovery and characterization of biosensors. Nat. Commun 2021, 12, 1437. [PubMed: 33664255]

(115). Hamers-Casterman C; Atarhouch T; Muyldermans S; Robinson G; Hammers C; Songa EB; Bendahman N; Hammers R Naturally occurring antibodies devoid of light chains. Nature 1993, 363, 446–448. [PubMed: 8502296]

(116). Muyldermans S Nanobodies: Natural Single-Domain Antibodies. Annu. Rev. Biochem 2013, 82, 775–797. [PubMed: 23495938]

(117). Wegner KD; Lindén S; Jin Z; Jennings TL; Khoulati RE; van Bergen en Henegouwen PMP; Hildebrandt N Nanobodies and Nanocrystals: Highly Sensitive Quantum Dot-Based Homogeneous FRET Immunoassay for Serum-Based EGFR Detection. Small 2014, 10, 734–740. [PubMed: 24115738]

(118). Irannejad R; Tomshine JC; Tomshine JR; Chevalier M; Mahoney JP; Steyaert J; Rasmussen SGF; Sunahara RK; El-Samad H; Huang B; von Zastrow M Conformational biosensors reveal GPCR signalling from endosomes. Nature 2013, 495, 534–538. [PubMed: 23515162]

(119). Beghein E; Gettemans J Nanobody Technology: A Versatile Toolkit for Microscopic Imaging, Protein–Protein Interaction Analysis, and Protein Function Exploration. Front. Immunol 2017, 8, 771. [PubMed: 28725224]

(120). Guo K; Wustoni S; Koklu A; Díaz-Galicia E; Moser M; Hama A; Alqahtani AA; Ahmad AN; Alhamlan FS; Shuaib M; Pain A; McCulloch I; Arold ST; Grünberg R; Inal S Rapid single-molecule detection of COVID-19 and MERS antigens via nanobody-functionalized organic electrochemical transistors. Nat. Biomed. Eng 2021, 5, 666–677. [PubMed: 34031558]

(121). Pardon E; Laeremans T; Triest S; Rasmussen SGF; Wohlkönig A; Ruf A; Muyldermans S; Hol WGJ; Kobilka BK; Steyaert J A general protocol for the generation of Nanobodies for structural biology. Nat. Protoc 2014, 9, 674–693. [PubMed: 24577359]

(122). Zimmermann I; Egloff P; Hutter CAJ; Kuhn BT; Bräuer P; Newstead S; Dawson RJP; Geertsma ER; Seeger MA Generation of synthetic nanobodies against delicate proteins. Nat. Protoc 2020, 15, 1707–1741. [PubMed: 32269381]

(123). Gao X; Teng X; Dai Y; Li J Rolling Circle Amplification-Assisted Flow Cytometry Approach for Simultaneous Profiling of Exosomal Surface Proteins. ACS Sens 2021, 6, 3611–3620. [PubMed: 34632781]

(124). Guo K; Li Z; Win A; Coreas R; Adkins GB; Cui X; Yan D; Cao M; Wang SE; Zhong W Calibration-free analysis of surface proteins on single extracellular vesicles enabled by DNA nanostructure. Biosens. Bioelectron 2021, 192, 113502. [PubMed: 34298496]

(125). Liu W; Li J; Wu Y; Xing S; Lai Y; Zhang G Targetinduced proximity ligation triggers recombinase polymerase amplification and transcription-mediated amplification to detect tumor-derived exosomes in nasopharyngeal carcinoma with high sensitivity. Biosens. Bioelectron 2018, 102, 204–210. [PubMed: 29145073]

(126). He Y; Wu Y; Wang Y; Wang X; Xing S; Li H; Guo S; Yu X; Dai S; Zhang G; Zeng M; Liu W Applying CRISPR/Cas13 to Construct Exosomal PD-L1 Ultrasensitive Biosensors for Dynamic Monitoring of Tumor Progression in Immunotherapy. Adv. Ther 2020, 3, 2000093.

(127). Lin Q; Huang Z; Ye X; Yang B; Fang X; Liu B; Chen H; Kong J Lab in a tube: Isolation, extraction, and isothermal amplification detection of exosomal long noncoding RNA of gastric cancer. Talanta 2021, 225, 122090. [PubMed: 33592799]

(128). Ali MM; Li F; Zhang Z; Zhang K; Kang D-K; Ankrum JA; Le XC; Zhao W Rolling circle amplification: a versatile tool for chemical biology, materials science and medicine. Chem. Soc. Rev 2014, 43, 3324–3341. [PubMed: 24643375]

(129). Li J; Eberwine J The successes and future prospects of the linear antisense RNA amplification methodology. Nat. Protoc 2018, 13, 811–818. [PubMed: 29599441]

(130). Xing S; Lu Z; Huang Q; Li H; Wang Y; Lai Y; He Y; Deng M; Liu W An ultrasensitive hybridization chain reaction-amplified CRISPR-Cas12a aptasensor for extracellular vesicle surface protein quantification. Theranostics 2020, 10, 10262–10273. [PubMed: 32929347]

(131). Houser B Bio-Rad's Bio-Plex® suspension array system, xMAP technology overview. Arch. Physiol. Biochem 2012, 118, 192–196. [PubMed: 22852821]

(132). Hu F; Zeng C; Long R; Miao Y; Wei L; Xu Q; Min W Supermultiplexed optical imaging and barcoding with engineered polyynes. Nat. Methods 2018, 15, 194–200. [PubMed: 29334378]

(133). Nguyen HQ; Baxter BC; Brower K; Diaz-Botia CA; DeRisi JL; Fordyce PM; Thorn KS Programmable Microfluidic Synthesis of Over One Thousand Uniquely Identifiable Spectral Codes. Adv. Opt. Mater 2017, 5, 1600548. [PubMed: 28936383]

(134). Zrazhevskiy P; Gao X Quantum dot imaging platform for single-cell molecular profiling. Nat. Commun 2013, 4, 1619. [PubMed: 23511483]

(135). Lu Y; Zhao J; Zhang R; Liu Y; Liu D; Goldys EM; Yang X; Xi P; Sunna A; Lu J; Shi Y; Leif RC; Huo Y; Shen J; Piper JA; Robinson JP; Jin D Tunable lifetime multiplexing using luminescent nanocrystals. Nat. Photonics 2014, 8, 32–36.

(136). Liang Y-C; Liu K-K; Wu X-Y; Lou Q; Sui L-Z; Dong L; Yuan K-J; Shan C-X Lifetime-Engineered Carbon Nanodots for Time Division Duplexing. Adv. Sci 2021, 8, 2003433.

(137). Giljohann DA; Mirkin CA Drivers of biodiagnostic development. Nature 2009, 462, 461–464. [PubMed: 19940916]

(138). Niemz A; Ferguson TM; Boyle DS Point-of-care nucleic acid testing for infectious diseases. Trends Biotechnol 2011, 29, 240–250. [PubMed: 21377748]

(139). Joung J; Ladha A; Saito M; Kim N-G; Woolley AE; Segel M; Barretto RPJ; Ranu A; Macrae RK; Faure G; Ioannidi EI; Krajeski RN; Bruneau R; Huang M-LW; Yu XG; Li JZ; Walker BD; Hung DT; Greninger AL; Jerome KR; et al. Detection of SARS-CoV-2 with SHERLOCK One-Pot Testing. N. Engl. J. Med 2020, 383, 1492–1494. [PubMed: 32937062]

(140). Craw P; Balachandran W Isothermal nucleic acid amplification technologies for point-of-care diagnostics: a critical review. Lab Chip 2012, 12, 2469–2486. [PubMed: 22592150]

(141). Venkatesan BM; Bashir R Nanopore sensors for nucleic acid analysis. Nat. Nanotechnol 2011, 6, 615–624. [PubMed: 21926981]

(142). Cai S; Sze JYY; Ivanov AP; Edel JB Small molecule electro-optical binding assay using nanopores. Nat. Commun 2019, 10, 1797. [PubMed: 30996223]

(143). Rosenstein JK; Wanunu M; Merchant CA; Drndic M; Shepard KL Integrated nanopore sensing platform with submicrosecond temporal resolution. Nat. Methods 2012, 9, 487–492. [PubMed: 22426489]

(144). Cai S; Pataillot-Meakin T; Shibakawa A; Ren R; Bevan CL; Ladame S; Ivanov AP; Edel JB Single-molecule amplification-free multiplexed detection of circulating microRNA cancer biomarkers from serum. Nat. Commun 2021, 12, 3515. [PubMed: 34112774]

(145). He L; Tessier DR; Briggs K; Tsangaris M; Charron M; McConnell EM; Lomovtsev D; Tabard-Cossa V Digital immunoassay for biomarker concentration quantification using solid-state nanopores. Nat. Commun 2021, 12, 5348. [PubMed: 34504071]

(146). Wanunu M; Dadosh T; Ray V; Jin J; McReynolds L; Drndić M Rapid electronic detection of probe-specific microRNAs using thin nanopore sensors. Nat. Nanotechnol 2010, 5, 807–814. [PubMed: 20972437]

(147). Danda G; Drndić M Two-dimensional nanopores and nanoporous membranes for ion and molecule transport. Curr. Opin. Biotechnol 2019, 55, 124–133. [PubMed: 30321759]

(148). Al Sulaiman D; Cadinu P; Ivanov AP; Edel JB; Ladame S Chemically Modified Hydrogel-Filled Nanopores: A Tunable Platform for Single-Molecule Sensing. Nano Lett 2018, 18, 6084–6093. [PubMed: 30105906]

(149). Manrao EA; Derrington IM; Laszlo AH; Langford KW; Hopper MK; Gillgren N; Pavlenok M; Niederweis M; Gundlach JH Reading DNA at single-nucleotide resolution with a mutant MspA nanopore and phi29 DNA polymerase. Nat. Biotechnol 2012, 30, 349–353. [PubMed: 22446694]

(150). Kaminski MM; Abudayyeh OO; Gootenberg JS; Zhang F; Collins JJ CRISPR-based diagnostics. Nat. Biomed. Eng 2021, 5, 643–656. [PubMed: 34272525]

(151). Gootenberg JS; Abudayyeh OO; Lee JW; Essletzbichler P; Dy AJ; Joung J; Verdine V; Donghia N; Daringer NM; Freije CA; Myhrvold C; Bhattacharyya RP; Livny J; Regev A; Koonin EV; Hung DT; Sabeti PC; Collins JJ; Zhang F Nucleic acid detection with CRISPR-Cas13a/C2c2. Science 2017, 356, 438–442. [PubMed: 28408723]

(152). Gootenberg JS; Abudayyeh OO; Kellner MJ; Joung J; Collins JJ; Zhang F Multiplexed and portable nucleic acid detection platform with Cas13, Cas12a, and Csm6. Science 2018, 360, 439–444. [PubMed: 29449508]

(153). Ackerman CM; Myhrvold C; Thakku SG; Freije CA; Metsky HC; Yang DK; Ye SH; Boehm CK; Kosoko-Thoroddsen T-SF; Kehe J; Nguyen TG; Carter A; Kulesa A; Barnes JR; Dugan VG; Hung DT; Blainey PC; Sabeti PC Massively multiplexed nucleic acid detection with Cas13. Nature 2020, 582, 277–282. [PubMed: 32349121]

(154). Hajian R; Balderston S; Tran T; deBoer T; Etienne J; Sandhu M; Wauford NA; Chung J-Y; Nokes J; Athaiya M; Paredes J; Peytavi R; Goldsmith B; Murthy N; Conboy IM; Aran K Detection of unamplified target genes via CRISPR–Cas9 immobilized on a graphene field-effect transistor. Nat. Biomed. Eng 2019, 3, 427–437. [PubMed: 31097816]

(155). Bruch R; Baaske J; Chatelle C; Meirich M; Madlener S; Weber W; Dincer C; Urban GA CRISPR/Cas13a-Powered Electrochemical Microfluidic Biosensor for Nucleic Acid Amplification-Free miRNA Diagnostics. Adv. Mater 2019, 31, 1905311.

(156). Chin LK; Son T; Hong J-S; Liu A-Q; Skog J; Castro CM; Weissleder R; Lee H; Im H Plasmonic Sensors for Extracellular Vesicle Analysis: From Scientific Development to Translational Research. ACS Nano 2020, 14, 14528–14548. [PubMed: 33119256]

(157). Im H; Shao H; Park YI; Peterson VM; Castro CM; Weissleder R; Lee H Label-free detection and molecular profiling of exosomes with a nano-plasmonic sensor. Nat. Biotechnol 2014, 32, 490–495. [PubMed: 24752081]

(158). Raghu D; Christodoulides JA; Christophersen M; Liu JL; Anderson GP; Robitaille M; Byers JM; Raphael MP Nanoplasmonic pillars engineered for single exosome detection. PLoS One 2018, 13, e0202773. [PubMed: 30142169]

(159). Liang K; Liu F; Fan J; Sun D; Liu C; Lyon CJ; Bernard DW; Li Y; Yokoi K; Katz MH; Koay EJ; Zhao Z; Hu Y Nanoplasmonic quantification of tumour-derived extracellular vesicles in plasma microsamples for diagnosis and treatment monitoring. Nat. Biomed. Eng 2017, 1, 0021. [PubMed: 28791195]

(160). Min J; Son T; Hong J-S; Cheah PS; Wegemann A; Murlidharan K; Weissleder R; Lee H; Im H Plasmon-Enhanced Biosensing for Multiplexed Profiling of Extracellular Vesicles. Adv. Biosyst 2020, 4, 2000003.

(161). Mathew DG; Beekman P; Lemay SG; Zuilhof H; Le Gac S; van der Wiel WG Electrochemical Detection of Tumor-Derived Extracellular Vesicles on Nanointerdigitated Electrodes. Nano Lett 2020, 20, 820–828. [PubMed: 31536360]

(162). Wang L; Wang X; Wu Y; Guo M; Gu C; Dai C; Kong D; Wang Y; Zhang C; Qu D; Fan C; Xie Y; Zhu Z; Liu Y; Wei D Rapid and ultrasensitive electromechanical detection of ions, biomolecules and SARS-CoV-2 RNA in unamplified samples. Nat. Biomed. Eng 2022, 6, 276–285. [PubMed: 35132229]

(163). Sabaté del Río J; Henry OYF; Jolly P; Ingber DE An antifouling coating that enables affinity-based electrochemical biosensing in complex biological fluids. Nat. Nanotechnol 2019, 14, 1143–1149. [PubMed: 31712665]

(164). Stuart T; Satija R Integrative single-cell analysis. Nat. Rev. Genet 2019, 20, 257–272. [PubMed: 30696980]

(165). Argelaguet R; Clark SJ; Mohammed H; Stapel LC; Krueger C; Kapourani C-A; Imaz-Rosshandler I; Lohoff T; Xiang Y; Hanna CW; Smallwood S; Ibarra-Soria X; Buettner F; Sanguinetti G; Xie W; Krueger F; Göttgens B; Rugg-Gunn PJ; Kelsey G; Dean W; et al. Multi-omics profiling of mouse gastrulation at single-cell resolution. Nature 2019, 576, 487–491. [PubMed: 31827285]

(166). Luo H-T; Zheng Y-Y; Tang J; Shao L-J; Mao Y-H; Yang W; Yang X-F; Li Y; Tian R-J; Li F-R Dissecting the multiomics atlas of the exosomes released by human lung adenocarcinoma stem-like cells. npj Genomic Med 2021, 6, 48.

(167). Lam SM; Zhang C; Wang Z; Ni Z; Zhang S; Yang S; Huang X; Mo L; Li J; Lee B; Mei M; Huang L; Shi M; Xu Z; Meng F-P; Cao W-J; Zhou M-J; Shi L; Chua GH; Li B; et al. A multi-omics investigation of the composition and function of extracellular vesicles along the temporal trajectory of COVID-19. Nat. Metab 2021, 3, 909–922. [PubMed: 34158670]

(168). Gayoso A; Steier Z; Lopez R; Regier J; Nazor KL; Streets A; Yosef N Joint probabilistic modeling of single-cell multiomic data with totalVI. Nat. Methods 2021, 18, 272–282. [PubMed: 33589839]

(169). Macaulay IC; Haerty W; Kumar P; Li YI; Hu TX; Teng MJ; Goolam M; Saurat N; Coupland P; Shirley LM; Smith M; Van der Aa N; Banerjee R; Ellis PD; Quail MA; Swerdlow HP; Zernicka-Goetz M; Livesey FJ; Ponting CP; Voet T G&T-seq: parallel sequencing of single-cell genomes and transcriptomes. Nat. Methods 2015, 12, 519–522. [PubMed: 25915121]

(170). Dey SS; Kester L; Spanjaard B; Bienko M; van Oudenaarden A Integrated genome and transcriptome sequencing of the same cell. Nat. Biotechnol 2015, 33, 285–289. [PubMed: 25599178]

(171). Angermueller C; Clark SJ; Lee HJ; Macaulay IC; Teng MJ; Hu TX; Krueger F; Smallwood SA; Ponting CP; Voet T; Kelsey G; Stegle O; Reik W Parallel single-cell sequencing links transcriptional and epigenetic heterogeneity. Nat. Methods 2016, 13, 229–232. [PubMed: 26752769]

(172). Darmanis S; Gallant CJ; Marinescu VD; Niklasson M; Segerman A; Flamourakis G; Fredriksson S; Assarsson E; Lundberg M; Nelander S; Westermark B; Landegren U Simultaneous Multiplexed Measurement of RNA and Proteins in Single Cells. Cell Rep 2016, 14, 380–389. [PubMed: 26748716]

(173). Stoeckius M; Hafemeister C; Stephenson W; Houck-Loomis B; Chattopadhyay PK; Swerdlow H; Satija R; Smibert P Simultaneous epitope and transcriptome measurement in single cells. Nat. Methods 2017, 14, 865–868. [PubMed: 28759029]

(174). Peterson VM; Zhang KX; Kumar N; Wong J; Li L; Wilson DC; Moore R; McClanahan TK; Sadekova S; Klappenbach JA Multiplexed quantification of proteins and transcripts in single cells. Nat. Biotechnol 2017, 35, 936–939. [PubMed: 28854175]

(175). Albayrak C; Jordi CA; Zechner C; Lin J; Bichsel CA; Khammash M; Tay S Digital Quantification of Proteins and mRNA in Single Mammalian Cells. Mol. Cell 2016, 61, 914–924. [PubMed: 26990994]

(176). Lin J; Jordi C; Son M; Van Phan H; Drayman N; Abasiyanik MF; Vistain L; Tu H-L; Tay S Ultra-sensitive digital quantification of proteins and mRNA in single cells. Nat. Commun 2019, 10, 3544. [PubMed: 31391463]

(177). Siedlik MJ; Yang Z; Kadam PS; Eberwine J; Issadore D Micro- and Nano-Devices for Studying Subcellular Biology. Small 2021, 17, 2005793.

(178). Frezza C; Cipolat S; Scorrano L Organelle isolation: functional mitochondria from mouse liver, muscle and cultured filroblasts. Nat. Protoc 2007, 2, 287–295. [PubMed: 17406588]

(179). Zand K; Pham T; Davila A; Wallace DC; Burke PJ Nanofluidic Platform for Single Mitochondria Analysis Using Fluorescence Microscopy. Anal. Chem 2013, 85, 6018–6025. [PubMed: 23678849]

(180). Kumar S; Wolken GG; Wittenberg NJ; Arriaga EA; Oh S-H Nanohole Array-Directed Trapping of Mammalian Mitochondria Enabling Single Organelle Analysis. Anal. Chem 2015, 87, 11973–11977. [PubMed: 26593329]

(181). Morris J; Na Y-J; Zhu H; Lee J-H; Giang H; Ulyanova AV; Baltuch GH; Brem S; Chen HI; Kung DK; Lucas TH; O'Rourke DM; Wolf JA; Grady MS; Sul J-Y; Kim J; Eberwine J Pervasive within-Mitochondrion Single-Nucleotide Variant Heteroplasmy as Revealed by Single-Mitochondrion Sequencing. Cell Rep 2017, 21, 2706–2713. [PubMed: 29212019]

(182). MacDonald JA; Bothun AM; Annis SN; Sheehan H; Ray S; Gao Y; Ivanov AR; Khrapko K; Tilly JL; Woods DC A nanoscale, multi-parametric flow cytometry-based platform to study mitochondrial heterogeneity and mitochondrial DNA dynamics. Commun. Biol 2019, 2, 258. [PubMed: 31312727]

(183). Sathyamurthy A; Johnson KR; Matson KJE; Dobrott CI; Li L; Ryba AR; Bergman TB; Kelly MC; Kelley MW; Levine AJ Massively Parallel Single Nucleus Transcriptional Profiling Defines Spinal Cord Neurons and Their Activity during Behavior. Cell Rep 2018, 22, 2216–2225. [PubMed: 29466745]

(184). Kim M; Franke V; Brandt B; Lowenstein ED; Schöwel V; Spuler S; Akalin A; Birchmeier C Single-nucleus transcriptomics reveals functional compartmentalization in syncytial skeletal muscle cells. Nat. Commun 2020, 11, 6375. [PubMed: 33311457]

(185). Slyper M; Porter CBM; Ashenberg O; Waldman J; Drokhlyansky E; Wakiro I; Smillie C; Smith-Rosario G; Wu J; Dionne D; Vigneau S; Jané-Valbuena J; Tickle TL; Napolitano S; Su M-J; Patel AG; Karlstrom A; Gritsch S; Nomura M; Waghray A; et al. A single-cell and single-nucleus RNA-Seq toolbox for fresh and frozen human tumors. Nat. Med 2020, 26, 792–802. [PubMed: 32405060]

(186). Macosko EZ; Basu A; Satija R; Nemesh J; Shekhar K; Goldman M; Tirosh I; Bialas AR; Kamitaki N; Martersteck EM; Trombetta JJ; Weitz DA; Sanes JR; Shalek AK; Regev A; McCarroll SA Highly Parallel Genome-wide Expression Profiling of Individual Cells Using Nanoliter Droplets. Cell. 2015, 161, 1202–1214. [PubMed: 26000488]

(187). Habib N; Avraham-Davidi I; Basu A; Burks T; Shekhar K; Hofree M; Choudhury SR; Aguet F; Gelfand E; Ardlie K; Weitz DA; Rozenblatt-Rosen O; Zhang F; Regev A Massively parallel single-nucleus RNA-seq with DroNc-seq. Nat. Methods 2017, 14, 955–958. [PubMed: 28846088]

(188). Gaublomme JT; Li B; McCabe C; Knecht A; Yang Y; Drokhlyansky E; Van Wittenberghe N; Waldman J; Dionne D; Nguyen L; De Jager PL; Yeung B; Zhao X; Habib N; Rozenblatt-Rosen O; Regev A Nuclei multiplexing with barcoded antibodies for single-nucleus genomics. Nat. Commun 2019, 10, 2907. [PubMed: 31266958]

(189). McGinnis CS; Patterson DM; Winkler J; Conrad DN; Hein MY; Srivastava V; Hu JL; Murrow LM; Weissman JS; Werb Z; Chow ED; Gartner ZJ MULTI-seq: sample multiplexing for single-cell RNA sequencing using lipid-tagged indices. Nat. Methods 2019, 16, 619–626. [PubMed: 31209384]

(190). Ko J; Baldassano SN; Loh P-L; Kording K; Litt B; Issadore D Machine learning to detect signatures of disease in liquid biopsies – a user's guide. Lab Chip. 2018, 18, 395–405. [PubMed: 29192299]

(191). Chen C; Zong S; Liu Y; Wang Z; Zhang Y; Chen B; Cui Y Profiling of Exosomal Biomarkers for Accurate Cancer Identification: Combining DNA-PAINT with Machine- Learning-Based Classification. Small. 2019, 15, 1901014.

(192). Kim H; Park S; Jeong IG; Song SH; Jeong Y; Kim C-S; Lee KH Noninvasive Precision Screening of Prostate Cancer by Urinary Multimarker Sensor and Artificial Intelligence Analysis. ACS Nano 2021, 15, 4054–4065. [PubMed: 33296173]

(193). Ko J; Bhagwat N; Yee SS; Ortiz N; Sahmoud A; Black T; Aiello NM; McKenzie L; O'Hara M; Redlinger C; Romeo J; Carpenter EL; Stanger BZ; Issadore D Combining Machine Learning and Nanofluidic Technology To Diagnose Pancreatic Cancer Using Exosomes. ACS Nano 2017, 11, 11182–11193. [PubMed: 29019651]

(194). Yang Z; LaRiviere MJ; Ko J; Till JE; Christensen T; Yee SS; Black TA; Tien K; Lin A; Shen H; Bhagwat N; Herman D; Adallah A; O'Hara MH; Vollmer CM; Katona BW; Stanger BZ; Issadore D; Carpenter EL A Multianalyte Panel Consisting of Extracellular Vesicle miRNAs and mRNAs, cfDNA, and CA19–9 Shows Utility for Diagnosis and Staging of Pancreatic Ductal Adenocarcinoma. Clin. Cancer Res 2020, 26, 3248–3258. [PubMed: 32299821]

(195). Shin H; Oh S; Hong S; Kang M; Kang D; Ji Y.-g.; Choi BH; Kang K-W; Jeong H; Park Y; Hong S; Kim HK; Choi Y Early-Stage Lung Cancer Diagnosis by Deep Learning-Based Spectroscopic Analysis of Circulating Exosomes. ACS Nano 2020, 14, 5435–5444. [PubMed: 32286793]

(196). McGranahan N; Swanton C Clonal Heterogeneity and Tumor Evolution: Past, Present, and the Future. Cell. 2017, 168, 613–628. [PubMed: 28187284]

(197). Snuderl M; Fazlollahi L; Le LP; Nitta M; Zhelyazkova BH; Davidson CJ; Akhavanfard S; Cahill DP; Aldape KD; Betensky RA; Louis DN; Iafrate AJ Mosaic Amplification of Multiple Receptor Tyrosine Kinase Genes in Glioblastoma. Cancer Cell. 2011, 20, 810–817. [PubMed: 22137795]

(198). Patel AP; Tirosh I; Trombetta JJ; Shalek AK; Gillespie SM; Wakimoto H; Cahill DP; Nahed BV; Curry WT; Martuza RL; Louis DN; Rozenblatt-Rosen O; Suva ML; Regev A; Bernstein BE Single-cell RNA-seq highlights intratumoral heterogeneity in primary glioblastoma. Science. 2014, 344, 1396–1401. [PubMed: 24925914]

(199). Landau DA; Carter SL; Stojanov P; McKenna A; Stevenson K; Lawrence MS; Sougnez C; Stewart C; Sivachenko A; Wang L; Wan Y; Zhang W; Shukla SA; Vartanov A; Fernandes SM; Saksena G; Cibulskis K; Tesar B; Gabriel S; Hacohen N; et al. Evolution and Impact of Subclonal Mutations in Chronic Lymphocytic Leukemia. Cell. 2013, 152, 714–726. [PubMed: 23415222]

(200). Fathi M; Joseph R; Adolacion JRT; Martinez-Paniagua M; An X; Gabrusiewicz K; Mani SA; Varadarajan N Single-Cell Cloning of Breast Cancer Cells Secreting Specific Subsets of Extracellular Vesicles. Cancers. 2021, 13, 4397. [PubMed: 34503207]

(201). Vagner T; Spinelli C; Minciacchi VR; Balaj L; Zandian M; Conley A; Zijlstra A; Freeman MR; Demichelis F; De S; Posadas EM; Tanaka H; Di Vizio D Large extracellular vesicles carry most of the tumour DNA circulating in prostate cancer patient plasma. J. Extracell. Vesicles 2018, 7, 1505403. [PubMed: 30108686]

(202). Garcia-Martin R; Wang G; Brandão BB; Zanotto TM; Shah S; Kumar Patel S; Schilling B; Kahn CR MicroRNA sequence codes for small extracellular vesicle release and cellular retention. Nature. 2022, 601, 446–451. [PubMed: 34937935]

(203). Ma C; Fan R; Ahmad H; Shi Q; Comin-Anduix B; Chodon T; Koya RC; Liu C-C; Kwong GA; Radu CG; Ribas A; Heath JR A clinical microchip for evaluation of single immune cells reveals high functional heterogeneity in phenotypically similar T cells. Nat. Med 2011, 17, 738–743. [PubMed: 21602800]

(204). Varadarajan N; Kwon DS; Law KM; Ogunniyi AO; Anahtar MN; Richter JM; Walker BD; Love JC Rapid, efficient functional characterization and recovery of HIV-specific human CD8+ T cells using microengraving. Proc. Natl. Acad. Sci. U. S. A 2012, 109, 3885–3890. [PubMed: 22355106]

(205). Ji Y; Qi D; Li L; Su H; Li X; Luo Y; Sun B; Zhang F; Lin B; Liu T; Lu Y Multiplexed profiling of single-cell extracellular vesicles secretion. Proc. Natl. Acad. Sci. U. S. A 2019, 116, 5979–5984. [PubMed: 30858327]

(206). Lee S; de Rutte J; Dimatteo R; Koo D; Di Carlo D Scalable Fabrication and Use of 3D Structured Microparticles Spatially Functionalized with Biomolecules. ACS Nano 2022, 16, 38–49. [PubMed: 34846855]

(207). de Rutte J; Dimatteo R; Archang MM; van Zee M; Koo D; Lee S; Sharrow AC; Krohl PJ; Mellody M; Zhu S; Eichenbaum JV; Kizerwetter M; Udani S; Ha K; Willson RC; Bertozzi AL; Spangler JB; Damoiseaux R; Di Carlo D Suspendable Hydrogel Nanovials for Massively Parallel Single-Cell Functional Analysis and Sorting. ACS Nano 2022, 16, 7242–7257. [PubMed: 35324146]

(208). Verweij FJ; Balaj L; Boulanger CM; Carter DRF; Compeer EB; D'Angelo G; El Andaloussi S; Goetz JG; Gross JC; Hyenne V; Krämer-Albers E-M; Lai CP; Loyer X; Marki A; Momma S; Nolte-'t Hoen ENM; Pegtel DM; Peinado H; Raposo G; Rilla K; et al. The power of imaging to understand extracellular vesicle biology in vivo. Nat. Methods 2021, 18, 1013–1026. [PubMed: 34446922]

(209). Men Y; Yelick J; Jin S; Tian Y; Chiang MSR; Higashimori H; Brown E; Jarvis R; Yang Y Exosome reporter mice reveal the involvement of exosomes in mediating neuron to astroglia communication in the CNS. Nat. Commun 2019, 10, 4136. [PubMed: 31515491]

(210). Sung BH; von Lersner A; Guerrero J; Krystofiak ES; Inman D; Pelletier R; Zijlstra A; Ponik SM; Weaver AM A live cell reporter of exosome secretion and uptake reveals pathfinding behavior of migrating cells. Nat. Commun 2020, 11, 2092. [PubMed: 32350252]

(211). Lai CP; Kim EY; Badr CE; Weissleder R; Mempel TR; Tannous BA; Breakefield XO Visualization and tracking of tumour extracellular vesicle delivery and RNA translation using multiplexed reporters. Nat. Commun 2015, 6, 7029. [PubMed: 25967391]

(212). Larson MH; Pan W; Kim HJ; Mauntz RE; Stuart SM; Pimentel M; Zhou Y; Knudsgaard P; Demas V; Aravanis AM; Jamshidi A A comprehensive characterization of the cell-free transcriptome reveals tissue- and subtype-specific biomarkers for cancer detection. Nat. Commun 2021, 12, 2357. [PubMed: 33883548]

(213). Vorperian SK; Moufarrej MN; Jones RC; Karkanias J; Krasnow M; Pisco AO; Quake SR; Salzman J; Yosef N; Bulthaup B; Brown P; Harper W; Hemenez M; Ponnusamy R; Salehi A;

Sanagavarapu BA; Spallino E; Aaron KA; Concepcion W; Gardner JM; et al. Cell types of origin of the cell-free transcriptome. Nat. Biotechnol 2022, 40, 855–861. [PubMed: 35132263]

(214). Zhu Q; Cheng L; Deng C; Huang L; Li J; Wang Y; Li M; Yang Q; Dong X; Su J; Lee LP; Liu F The genetic source tracking of human urinary exosomes. Proc. Natl. Acad. Sci. U. S. A 2021, 118, e2108876118. [PubMed: 34663731]

(215). Larssen P; Wik L; Czarnewski P; Eldh M; Löf L; Ronquist KG; Dubois L; Freyhult E; Gallant CJ; Oelrich J; Larsson A; Ronquist G; Villablanca EJ; Landegren U; Gabrielsson S; Kamali-Moghaddam M Tracing Cellular Origin of Human Exosomes Using Multiplex Proximity Extension Assays. Mol. Cell. Proteomics 2017, 16, 502–511. [PubMed: 28111361]

(216). D'Souza AL; Tseng JR; Pauly KB; Guccione S; Rosenberg J; Gambhir SS; Glazer GM A strategy for blood biomarker amplification and localization using ultrasound. Proc. Natl. Acad. Sci. U. S. A 2009, 106, 17152–17157. [PubMed: 19805109]

(217). Hori SS; Gambhir SS Mathematical Model Identifies Blood Biomarker–Based Early Cancer Detection Strategies and Limitations. Sci. Transl. Med 2011, 3, 109ra116.

(218). Hori SS; Lutz AM; Paulmurugan R; Gambhir SS A Model-Based Personalized Cancer Screening Strategy for Detecting Early-Stage Tumors Using Blood-Borne Biomarkers. Cancer Res. 2017, 77, 2570–2584. [PubMed: 28283654]

(219). Kwong GA; von Maltzahn G; Murugappan G; Abudayyeh O; Mo S; Papayannopoulos IA; Sverdlov DY; Liu SB; Warren AD; Popov Y; Schuppan D; Bhatia SN Massencoded synthetic biomarkers for multiplexed urinary monitoring of disease. Nat. Biotechnol 2013, 31, 63–70. [PubMed: 23242163]

(220). Shao H; Im H; Castro CM; Breakefield X; Weissleder R; Lee H New Technologies for Analysis of Extracellular Vesicles. Chem. Rev 2018, 118, 1917–1950. [PubMed: 29384376]

(221). Jeppesen DK; Fenix AM; Franklin JL; Higginbotham JN; Zhang Q; Zimmerman LJ; Liebler DC; Ping J; Liu Q; Evans R; Fissell WH; Patton JG; Rome LH; Burnette DT; Coffey RJ Reassessment of Exosome Composition. Cell. 2019, 177, 428. [PubMed: 30951670]

(222). Mathieu M; Névo N; Jouve M; Valenzuela JI; Maurin M; Verweij FJ; Palmulli R; Lankar D; Dingli F; Loew D; Rubinstein E; Boncompain G; Perez F; Théry C Specificities of exosome versus small ectosome secretion revealed by live intracellular tracking of CD63 and CD9. Nat. Commun 2021, 12, 4389. [PubMed: 34282141]

(223). Théry C; Witwer KW; Aikawa E; Alcaraz MJ; Anderson JD; Andriantsitohaina R; Antoniou A; Arab T; Archer F; Atkin-Smith GK; Ayre DC; Bach J-M; Bachurski D; Baharvand H; Balaj L; Baldacchino S; Bauer NN; Baxter AA; Bebawy M; Beckham C; et al. Minimal information for studies of extracellular vesicles 2018 (MISEV2018): a position statement of the International Society for Extracellular Vesicles and update of the MISEV2014 guidelines. J. Extracell. Vesicles 2018, 7, 1535750. [PubMed: 30637094]

(224). Libregts SFWM; Arkesteijn GJA; Németh A; Nolte-'t Hoen ENM; Wauben MHM Flow cytometric analysis of extracellular vesicle subsets in plasma: impact of swarm by particles of non-interest. J. Thromb. Haemostasis 2018, 16, 1423–1436. [PubMed: 29781099]

(225). Böing AN; van der Pol E; Grootemaat AE; Coumans FAW; Sturk A; Nieuwland R Single-step isolation of extracellular vesicles by size-exclusion chromatography. J. Extracell. Vesicles 2014, 3, 23430.

(226). Simonsen JB What Are We Looking At? Extracellular Vesicles, Lipoproteins, or Both? Circ. Res 2017, 121, 920–922. [PubMed: 28963190]

(227). Xu R; Greening DW; Zhu H-J; Takahashi N; Simpson RJ Extracellular vesicle isolation and characterization: toward clinical application. J. Clin. Invest 2016, 126, 1152–1162. [PubMed: 27035807]

(228). Wu Y; Tilley RD; Gooding JJ Challenges and Solutions in Developing Ultrasensitive Biosensors. J. Am. Chem. Soc 2019, 141, 1162–1170. [PubMed: 30463401]

(229). Welsh JA; Pol E; Bettin BA; Carter DRF; Hendrix A; Lenassi M; Langlois M-A; Llorente A; Nes AS; Nieuwland R; Tang V; Wang L; Witwer KW; Jones JC Towards defining reference materials for measuring extracellular vesicle refractive index, epitope abundance, size and concentration. J. Extracell. Vesicles 2020, 9, 1816641. [PubMed: 33062218]

(230). Geeurickx E; Tulkens J; Dhondt B; Van Deun J; Lippens L; Vergauwen G; Heyrman E; De Sutter D; Gevaert K; Impens F; Miinalainen I; Van Bockstal P-J; De Beer T; Wauben MHM; Nolte-'t-Hoen ENM; Bloch K; Swinnen JV; van der Pol E; Nieuwland R; Braems G; et al. The generation and use of recombinant extracellular vesicles as biological reference material. Nat. Commun 2019, 10, 3288. [PubMed: 31337761]

(231). Geeurickx E; Lippens L; Rappu P; De Geest BG; De Wever O; Hendrix A Recombinant extracellular vesicles as biological reference material for method development, data normalization and assessment of (pre-)analytical variables. Nat. Protoc 2021, 16, 603–633. [PubMed: 33452501]

(232). Van Deun J; Mestdagh P; Agostinis P; Akay Ö; Anand S; Anckaert J; Martinez ZA; Baetens T; Beghein E; Bertier L; Berx G; Boere J; Boukouris S; Bremer M; Buschmann D; Byrd JB; Casert C; Cheng L; Cmoch A; Daveloose D; et al. EV-TRACK: transparent reporting and centralizing knowledge in extracellular vesicle research. Nat. Methods 2017, 14, 228–232. [PubMed: 28245209]

(233). Mellacheruvu D; Wright Z; Couzens AL; Lambert J-P; St-Denis NA; Li T; Miteva YV; Hauri S; Sardiu ME; Low TY; Halim VA; Bagshaw RD; Hubner NC; al-Hakim A; Bouchard A; Faubert D; Fermin D; Dunham WH; Goudreault M; Lin Z-Y; et al. The CRAPome: a contaminant repository for affinity purification–mass spectrometry data. Nat. Methods 2013, 10, 730–736. [PubMed: 23921808]

(234). Keerthikumar S; Chisanga D; Ariyaratne D; Al Saffar H; Anand S; Zhao K; Samuel M; Pathan M; Jois M; Chilamkurti N; Gangoda L; Mathivanan S ExoCarta: A Web-Based Compendium of Exosomal Cargo. J. Mol. Biol 2016, 428, 688–692. [PubMed: 26434508]

(235). Pathan M; Fonseka P; Chitti SV; Kang T; Sanwlani R; Van Deun J; Hendrix A; Mathivanan S Vesiclepedia 2019: a compendium of RNA, proteins, lipids and metabolites in extracellular vesicles. Nucleic Acids Res. 2019, 47, D516–D519. [PubMed: 30395310]

(236). Kim AS; Bartley AN; Bridge JA; Kamel-Reid S; Lazar AJ; Lindeman NI; Long TA; Merker JD; Rai AJ; Rimm DL; Rothberg PG; Vasalos P; Moncur JT Comparison of Laboratory-Developed Tests and FDA-Approved Assays for BRAF, EGFR, and KRAS Testing. JAMA Oncol. 2018, 4, 838–841. [PubMed: 29242895]

(237). Genzen JR Regulation of Laboratory-Developed Tests: A Clinical Laboratory Perspective. Am. J. Clin. Pathol 2019, 152, 122–131. [PubMed: 31242284]

(238). Yekula A; Muralidharan K; Kang KM; Wang L; Balaj L; Carter BS From laboratory to clinic: Translation of extracellular vesicle based cancer biomarkers. Methods. 2020, 177, 58–66. [PubMed: 32061674]

(239). McKiernan J; Donovan MJ; O'Neill V; Bentink S; Noerholm M; Belzer S; Skog J; Kattan MW; Partin A; Andriole G; Brown G; Wei JT; Thompson IM Jr.; Carroll P A Novel Urine Exosome Gene Expression Assay to Predict High-grade Prostate Cancer at Initial Biopsy. JAMA Oncol. 2016, 2, 882–889. [PubMed: 27032035]

(240). McKiernan J; Donovan MJ; Margolis E; Partin A; Carter B; Brown G; Torkler P; Noerholm M; Skog J; Shore N; Andriole G; Thompson I; Carroll P A Prospective Adaptive Utility Trial to Validate Performance of a Novel Urine Exosome Gene Expression Assay to Predict High-grade Prostate Cancer in Patients with Prostate-specific Antigen 2– 10ng/mL at Initial Biopsy. Eur. Urol 2018, 74, 731–738. [PubMed: 30237023]

(241). Loeb S; Vellekoop A; Ahmed HU; Catto J; Emberton M; Nam R; Rosario DJ; Scattoni V; Lotan Y Systematic Review of Complications of Prostate Biopsy. Eur. Urol 2013, 64, 876–892. [PubMed: 23787356]

(242). Margolis E; Brown G; Partin A; Carter B; McKiernan J; Tutrone R; Torkler P; Fischer C; Tadigotla V; Noerholm M; Donovan MJ; Skog J Predicting high-grade prostate cancer at initial biopsy: clinical performance of the ExoDx (EPI) Prostate Intelliscore test in three independent prospective studies. Prostate Cancer Prostatic Dis. 2022, 25, 296–301. [PubMed: 34593984]

(243). Weissleder R; Lee H; Ko J; Pittet MJ COVID-19 diagnostics in context. Sci. Transl. Med 2020, 12, eabc1931. [PubMed: 32493791]

(244). Dincer C; Bruch R; Kling A; Dittrich PS; Urban GA Multiplexed Point-of-Care Testing - xPOCT. Trends Biotechnol. 2017, 35, 728–742. [PubMed: 28456344]

(245). Ramshani Z; Zhang C; Richards K; Chen L; Xu G; Stiles BL; Hill R; Senapati S; Go DB; Chang H-C Extracellular vesicle microRNA quantification from plasma using an integrated microfluidic device. Commun. Biol 2019, 2, 189. [PubMed: 31123713]

(246). Jahani Y; Arvelo ER; Yesilkoy F; Koshelev K; Cianciaruso C; De Palma M; Kivshar Y; Altug H Imaging-based spectrometer-less optofluidic biosensors based on dielectric metasurfaces for detecting extracellular vesicles. Nat. Commun 2021, 12, 3246. [PubMed: 34059690]

(247). Yelleswarapu V; Buser JR; Haber M; Baron J; Inapuri E; Issadore D Mobile platform for rapid sub–picogram-permilliliter, multiplexed, digital droplet detection of proteins. Proc. Natl. Acad. Sci. U. S. A 2019, 116, 4489–4495. [PubMed: 30765530]

(248). Chin CD; Laksanasopin T; Cheung YK; Steinmiller D; Linder V; Parsa H; Wang J; Moore H; Rouse R; Umviligihozo G; Karita E; Mwambarangwe L; Braunstein SL; van de Wijgert J; Sahabo R; Justman JE; El-Sadr W; Sia SK Microfluidics-based diagnostics of infectious diseases in the developing world. Nat. Med 2011, 17, 1015–1019. [PubMed: 21804541]

(249). Park J; Park JS; Huang C-H; Jo A; Cook K; Wang R; Lin H-Y; Van Deun J; Li H; Min J; Wang L; Yoon G; Carter BS; Balaj L; Choi G-S; Castro CM; Weissleder R; Lee H An integrated magneto-electrochemical device for the rapid profiling of tumour extracellular vesicles from blood plasma. Nat. Biomed. Eng 2021, 5, 678–689. [PubMed: 34183802]

(250). Peinado H; Alečković M; Lavotshkin S; Matei I; Costa-Silva B; Moreno-Bueno G; Hergueta-Redondo M; Williams C; García-Santos G; Ghajar CM; Nitadori-Hoshino A; Hoffman C; Badal K; Garcia BA; Callahan MK; Yuan J; Martins VR; Skog J; Kaplan RN; Brady MS; et al. Melanoma exosomes educate bone marrow progenitor cells toward a pro-metastatic phenotype through MET. Nat. Med 2012, 18, 883–891. [PubMed: 22635005]

(251). Sun N; Lee Y-T; Zhang RY; Kao R; Teng P-C; Yang Y; Yang P; Wang JJ; Smalley M; Chen P-J; Kim M; Chou S-J; Bao L; Wang J; Zhang X; Qi D; Palomique J; Nissen N; Han S-HB; Sadeghi S; et al. Purification of HCC-specific extracellular vesicles on nanosubstrates for early HCC detection by digital scoring. Nat. Commun 2020, 11, 4489. [PubMed: 32895384]

(252). Zhang P; Wu X; Gardashova G; Yang Y; Zhang Y; Xu L; Zeng Y Molecular and functional extracellular vesicle analysis using nanopatterned microchips monitors tumor progression and metastasis. Sci. Transl. Med 2020, 12, eaaz2878. [PubMed: 32522804]

(253). Shao H; Chung J; Balaj L; Charest A; Bigner DD; Carter BS; Hochberg FH; Breakefield XO; Weissleder R; Lee H Protein typing of circulating microvesicles allows real-time monitoring of glioblastoma therapy. Nat. Med 2012, 18, 1835–1840. [PubMed: 23142818]

(254). Huang M; Yang J; Wang T; Song J; Xia J; Wu L; Wang W; Wu Q; Zhu Z; Song Y; Yang C Homogeneous, Low-volume, Efficient, and Sensitive Quantitation of Circulating Exosomal PD-L1 for Cancer Diagnosis and Immunotherapy Response Prediction. Angew. Chem., Int. Ed 2020, 59, 4800–4805.

(255). Tian F; Zhang S; Liu C; Han Z; Liu Y; Deng J; Li Y; Wu X; Cai L; Qin L; Chen Q; Yuan Y; Liu Y; Cong Y; Ding B; Jiang Z; Sun J Protein analysis of extracellular vesicles to monitor and predict therapeutic response in metastatic breast cancer. Nat. Commun 2021, 12, 2536. [PubMed: 33953198]

(256). Shi A; Kasumova GG; Michaud WA; Cintolo-Gonzalez J; Diaz-Martinez M; Ohmura J; Mehta A; Chien I; Frederick DT; Cohen S; Plana D; Johnson D; Flaherty KT; Sullivan RJ; Kellis M; Boland GM Plasma-derived extracellular vesicle analysis and deconvolution enable prediction and tracking of melanoma checkpoint blockade outcome. Sci. Adv 2020, 6, eabb3461. [PubMed: 33188016]

(257). Shao H; Chung J; Lee K; Balaj L; Min C; Carter BS; Hochberg FH; Breakefield XO; Lee H; Weissleder R Chipbased analysis of exosomal mRNA mediating drug resistance in glioblastoma. Nat. Commun 2015, 6, 6999. [PubMed: 25959588]

(258). Zhou J; Jangili P; Son S; Ji MS; Won M; Kim JS Fluorescent Diagnostic Probes in Neurodegenerative Diseases. Adv. Mater 2020, 32, 2001945.

(259). Matsumoto J; Stewart T; Sheng L; Li N; Bullock K; Song N; Shi M; Banks WA; Zhang J Transmission of α-synuclein-containing erythrocyte-derived extracellular vesicles across the blood-brain barrier via adsorptive mediated transcytosis: another mechanism for initiation and progression of Parkinson's disease? Acta Neuropathol. Commun 2017, 5, 71. [PubMed: 28903781]

(260). Morad G; Carman CV; Hagedorn EJ; Perlin JR; Zon LI; Mustafaoglu N; Park T-E; Ingber DE; Daisy CC; Moses MA Tumor-Derived Extracellular Vesicles Breach the Intact Blood–Brain Barrier via Transcytosis. ACS Nano 2019, 13, 13853–13865. [PubMed: 31479239]

(261). Mustapic M; Eitan E; Werner JK; Berkowitz ST; Lazaropoulos MP; Tran J; Goetzl EJ; Kapogiannis D Plasma Extracellular Vesicles Enriched for Neuronal Origin: A Potential Window into Brain Pathologic Processes. Front. Neurosci 2017, 11, 278. [PubMed: 28588440]

(262). Rabinstein AA Update on Treatment of Acute Ischemic Stroke. Continuum 2020, 26, 268–286. [PubMed: 32224752]

(263). Burrello J; Bianco G; Burrello A; Manno C; Maulucci F; Pileggi M; Nannoni S; Michel P; Bolis S; Melli G; Vassalli G; Albers GW; Cianfoni A; Barile L; Cereda CW Extracellular Vesicle Surface Markers as a Diagnostic Tool in Transient Ischemic Attacks. Stroke. 2021, 52, 3335–3347. [PubMed: 34344167]

(264). Kalani MYS; Alsop E; Meechoovet B; Beecroft T; Agrawal K; Whitsett TG; Huentelman MJ; Spetzler RF; Nakaji P; Kim S; Van Keuren-Jensen K Extracellular microRNAs in blood differentiate between ischaemic and haemorrhagic stroke subtypes. J. Extracell. Vesicles 2020, 9, 1713540. [PubMed: 32128071]

(265). Wijerathne H; Witek MA; Jackson JM; Brown V; Hupert ML; Herrera K; Kramer C; Davidow AE; Li Y; Baird AE; Murphy MC; Soper SA Affinity enrichment of extracellular vesicles from plasma reveals mRNA changes associated with acute ischemic stroke. Commun. Biol 2020, 3, 613. [PubMed: 33106557]

(266). Ibsen SD; Wright J; Lewis JM; Kim S; Ko S-Y; Ong J; Manouchehri S; Vyas A; Akers J; Chen CC; Carter BS; Esener SC; Heller MJ Rapid Isolation and Detection of Exosomes and Associated Biomarkers from Plasma. ACS Nano 2017, 11, 6641–6651. [PubMed: 28671449]

(267). Spudich S; Nath A Nervous system consequences of COVID-19. Science. 2022, 375, 267–269. [PubMed: 35050660]

(268). Thakur KT; Miller EH; Glendinning MD; Al-Dalahmah O; Banu MA; Boehme AK; Boubour AL; Bruce SS; Chong AM; Claassen J; Faust PL; Hargus G; Hickman RA; Jambawalikar S; Khandji AG; Kim CY; Klein RS; Lignelli-Dipple A; Lin C-C; Liu Y; et al. COVID-19 neuropathology at Columbia University Irving Medical Center/New York Presbyterian Hospital. Brain. 2021, 144, 2696–2708. [PubMed: 33856027]

(269). Song E; Bartley CM; Chow RD; Ngo TT; Jiang R; Zamecnik CR; Dandekar R; Loudermilk RP; Dai Y; Liu F; Sunshine S; Liu J; Wu W; Hawes IA; Alvarenga BD; Huynh T; McAlpine L; Rahman N-T; Geng B; Chiarella J; et al. Divergent and self-reactive immune responses in the CNS of COVID-19 patients with neurological symptoms. Cell Rep. Med 2021, 2, 100288. [PubMed: 33969321]

(270). Lee M-H; Perl DP; Nair G; Li W; Maric D; Murray H; Dodd SJ; Koretsky AP; Watts JA; Cheung V; Masliah E; Horkayne-Szakaly I; Jones R; Stram MN; Moncur J; Hefti M; Folkerth RD; Nath A Microvascular Injury in the Brains of Patients with Covid-19. N. Engl. J. Med 2021, 384, 481–483. [PubMed: 33378608]

(271). Frontera JA; Boutajangout A; Masurkar AV; Betensky RA; Ge Y; Vedvyas A; Debure L; Moreira A; Lewis A; Huang J; Thawani S; Balcer L; Galetta S; Wisniewski T Comparison of serum neurodegenerative biomarkers among hospitalized COVID-19 patients versus non-COVID subjects with normal cognition, mild cognitive impairment, or Alzheimer's dementia. Alzheimer's & Dementia 2022, 18, 899–910.

(272). DeKosky ST; Kochanek PM; Valadka AB; Clark RSB; Chou SHY; Au AK; Horvat C; Jha RM; Mannix R; Wisniewski SR; Wintermark M; Rowell SE; Welch RD; Lewis L; House S; Tanzi RE; Smith DR; Vittor AY; Denslow ND; Davis MD; et al. Blood Biomarkers for Detection of Brain Injury in COVID-19 Patients. J. Neurotrauma 2021, 38, 1–43. [PubMed: 33115334]

(273). Ko J; Hemphill M; Yang Z; Beard K; Sewell E; Shallcross J; Schweizer M; Sandsmark DK; Diaz-Arrastia R; Kim J; Meaney D; Issadore D Multi-Dimensional Mapping of Brain-Derived Extracellular Vesicle MicroRNA Biomarker for Traumatic Brain Injury Diagnostics. J. Neurotrauma 2020, 37, 2424–2434. [PubMed: 30950328]

(274). Beard K; Yang Z; Haber M; Flamholz M; Diaz-Arrastia R; Sandsmark D; Meaney DF; Issadore D Extracellular vesicles as distinct biomarker reservoirs for mild traumatic brain injury diagnosis. Brain Commun. 2021, 3, fcab151. [PubMed: 34622206]

(275). Marder SR; Cannon TD Schizophrenia. N. Engl. J. Med 2019, 381, 1753–1761. [PubMed: 31665579]

(276). Lieberman JA; Small SA; Girgis RR Early Detection and Preventive Intervention in Schizophrenia: From Fantasy to Reality. Am. J. Psychiatry 2019, 176, 794–810. [PubMed: 31569988]

(277). Khadimallah I; Jenni R; Cabungcal J-H; Cleusix M; Fournier M; Beard E; Klauser P; Knebel J-F; Murray MM; Retsa C; Siciliano M; Spencer KM; Steullet P; Cuenod M; Conus P; Do KQ Mitochondrial, exosomal miR137-COX6A2 and gamma synchrony as biomarkers of parvalbumin interneurons, psychopathology, and neurocognition in schizophrenia. Mol. Psychiatry 2021, 1192–1204. [PubMed: 34686767]

(278). Rush AJ; Trivedi MH; Wisniewski SR; Nierenberg AA; Stewart JW; Warden D; Niederehe G; Thase ME; Lavori PW; Lebowitz BD; McGrath PJ; Rosenbaum JF; Sackeim HA; Kupfer DJ; Luther J; Fava M Acute and Longer-Term Outcomes in Depressed Outpatients Requiring One or Several Treatment Steps: A STAR*D Report. Am. J. Psychiatry 2006, 163, 1905–1917. [PubMed: 17074942]

(279). Gururajan A; Reif A; Cryan JF; Slattery DA The future of rodent models in depression research. Nat. Rev. Neurosci 2019, 20, 686–701. [PubMed: 31578460]

(280). Raison CL; Rutherford RE; Woolwine BJ; Shuo C; Schettler P; Drake DF; Haroon E; Miller AH A Randomized Controlled Trial of the Tumor Necrosis Factor Antagonist Infliximab for Treatment-Resistant Depression: The Role of Baseline Inflammatory Biomarkers. JAMA Psychiatry. 2013, 70, 31–41. [PubMed: 22945416]

(281). Lopez JP; Lim R; Cruceanu C; Crapper L; Fasano C; Labonte B; Maussion G; Yang JP; Yerko V; Vigneault E; El Mestikawy S; Mechawar N; Pavlidis P; Turecki G miR-1202 is a primate-specific and brain-enriched microRNA involved in major depression and antidepressant treatment. Nat. Med 2014, 20, 764–768. [PubMed: 24908571]

(282). Lopez JP; Fiori LM; Cruceanu C; Lin R; Labonte B; Cates HM; Heller EA; Vialou V; Ku SM; Gerald C; Han M-H; Foster J; Frey BN; Soares CN; Müller DJ; Farzan F; Leri F; MacQueen GM; Feilotter H; Tyryshkin K; et al. MicroRNAs 146a/b-5 and 425–3p and 24–3p are markers of antidepressant response and regulate MAPK/Wnt-system genes. Nat. Commun 2017, 8, 15497. [PubMed: 28530238]

(283). Saeedi S; Nagy C; Ibrahim P; Théroux J-F; Wakid M; Fiori LM; Yang J; Rotzinger S; Foster JA; Mechawar N; Kennedy SH; Turecki G Neuron-derived extracellular vesicles enriched from plasma show altered size and miRNA cargo as a function of antidepressant drug response. Mol. Psychiatry 2021, 26, 7417–7424. [PubMed: 34385599]

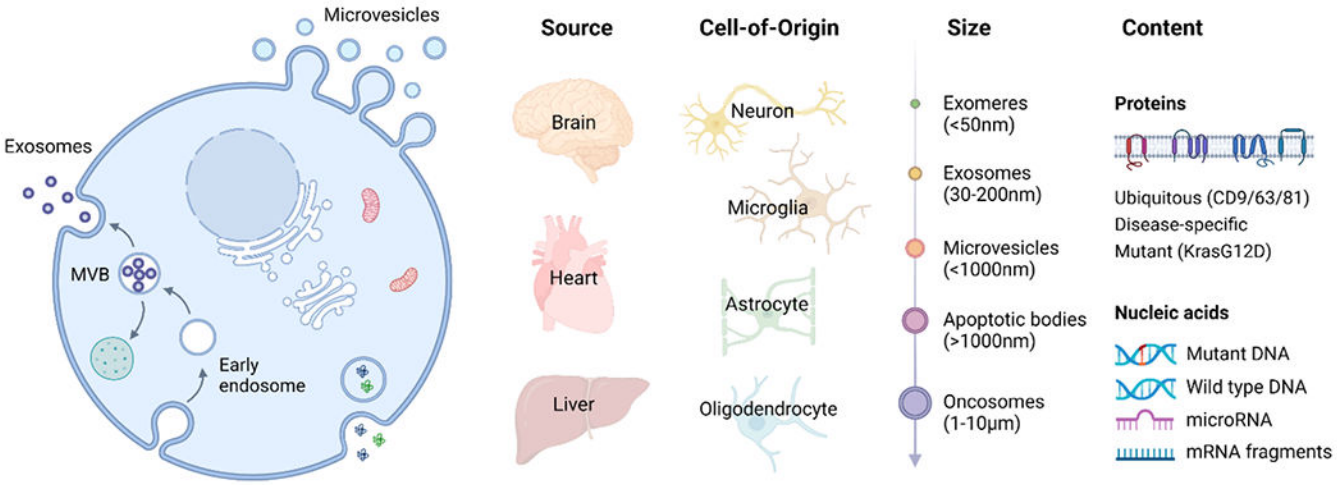

Figure 1.

Multiparametric heterogeneity of EVs. EVs are generated from a range of biogenesis mechanisms, and the most studied EV subsets—exosomes and microvesicles—originate as intraluminal vesicles formed within multivesicular bodies or bud directly from the plasma membrane, respectively. From diverse organ/tissue sources, different cell types altogether secrete a heterogeneous expression of EVs that drive biological responses in health and disease, which can be profiled according to their relative abundance and diversity of size classes (nm to ***μ***m scale) and molecular content (proteins and nucleic acids).

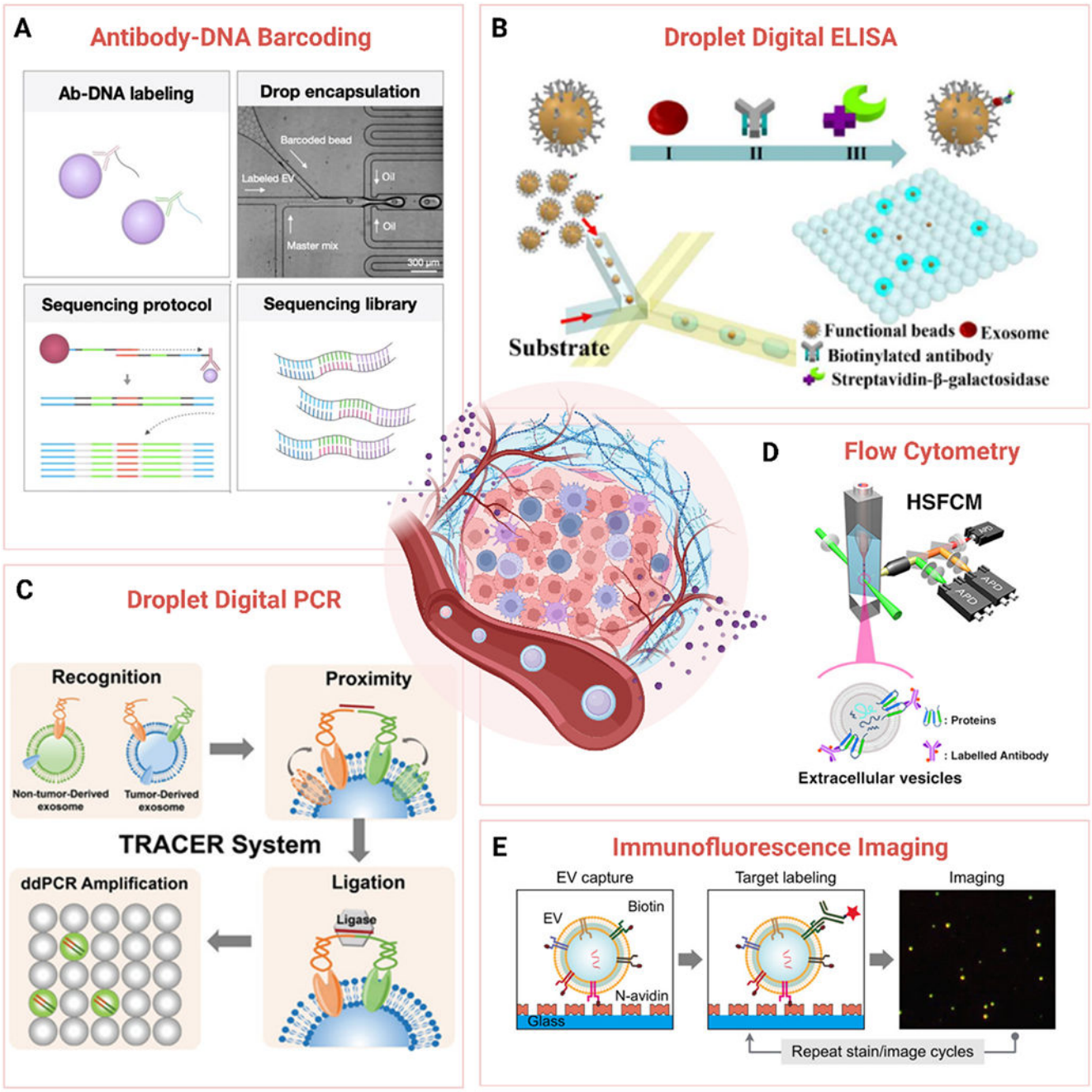

Figure 2.

Major classes of single-EV label-based assays. (A) Antibody (Ab)–DNA barcoding: single EVs are labeled with Ab–DNA barcodes that undergo droplet encapsulation and PCR amplification and, subsequently, sequencing to read out protein identity. Reprinted from ref 55. Copyright 2021 American Chemical Society. (B) Droplet digital ELISA: single EVs are immobilized by sandwich ELISA immunocomplexes and incorporated into droplets for digital analysis by a fluorescence readout. Reprinted from ref 62. Copyright 2018 American Chemical Society. (C) Droplet digital PCR: EVs are labeled with aptamer probes in close

proximity that ligate together. Ligation products are amplified and sorted into droplets, and target expression is readout by fluorescence. Reprinted with permission from ref 70. Copyright 2021 Wiley-VCH. (D) Flow cytometry: EVs are labeled with fluorophore-tagged Abs that label surface proteins and passed through a flow cytometer, enabling a readout of scattered light for each particle. Reprinted from ref 78. Copyright 2018 American Chemical Society. (E) Immunofluorescence imaging: single EVs are immobilized on glass within a microfluidic channel and are repeatedly immunostained and imaged for multiple rounds. Reprinted from ref 35. Copyright 2018 American Chemical Society.

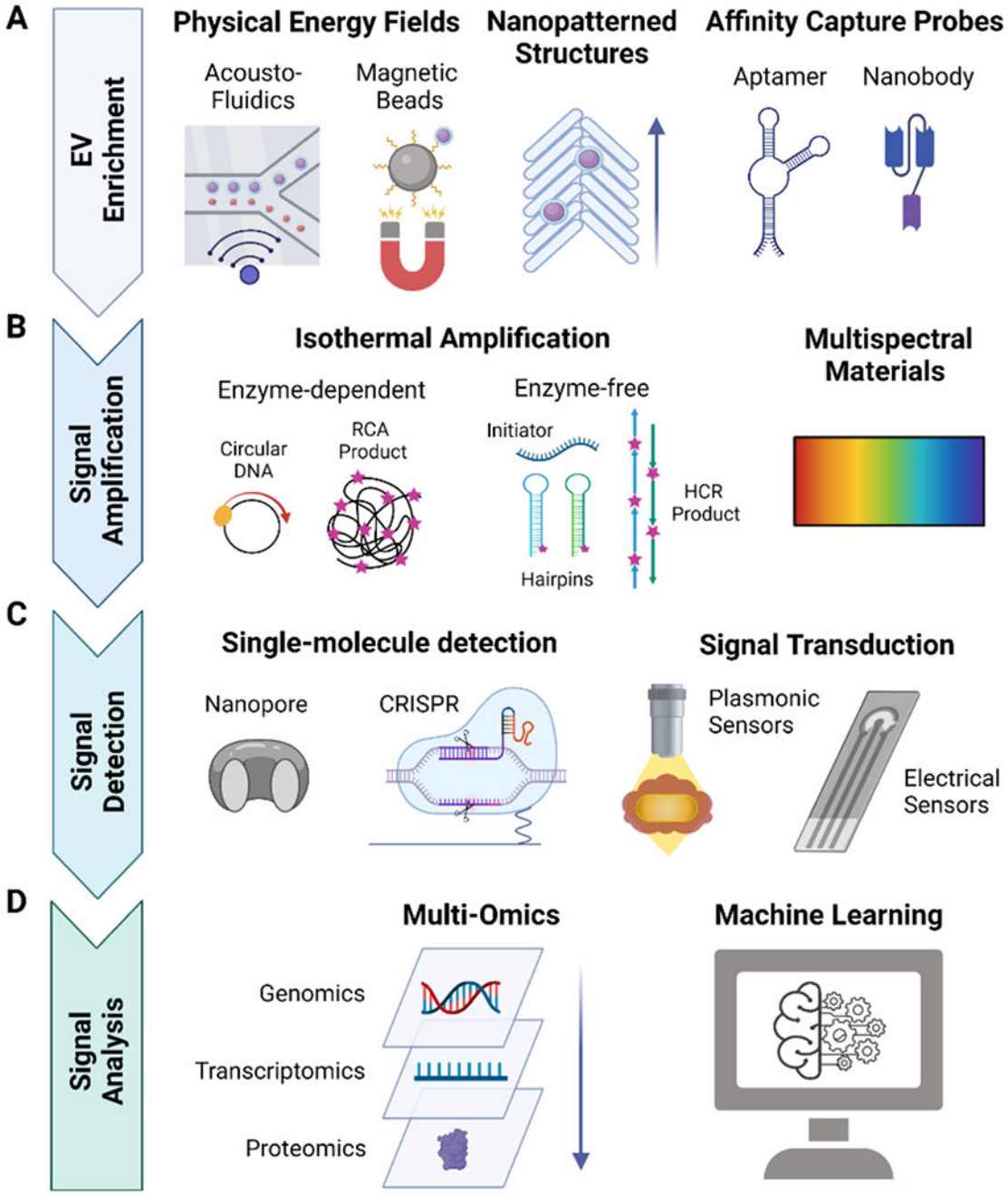

Figure 3.

Future design opportunities for single EV assays. Optimizing the sensitivity, throughput, and multiplexing capacity of single EV assays requires targeting keys areas of the assay pipeline: EV enrichment, signal amplification, signal detection, and signal analysis. (A) EV enrichment can include manipulating physical energy fields such as ultrasound standing waves in microfluidics (acousto-fluidics) or EV-captured magnetic beads (left); nanopatterning structures to capture EVs (middle); and developing functional affinity capture probes (aptamers and nanobodies) that can replace Abs (right). (B) Signal

amplification involves incorporating DNA-assisted isothermal amplification (RCA and HCR) (left) and overcoming the optical multiplexed ceiling with multispectral materials (right). (C) Signal detection involves bypassing preamplification requirements such as nanopores or CRISPR-based sensors (left) or converting target signal into quantifiable readouts (plasmonic or electrical sensors) (right). (D) Signal analysis involves integrating omics approaches (left) and applying machine learning algorithms (right) to interpret volumes of data for single EVs.

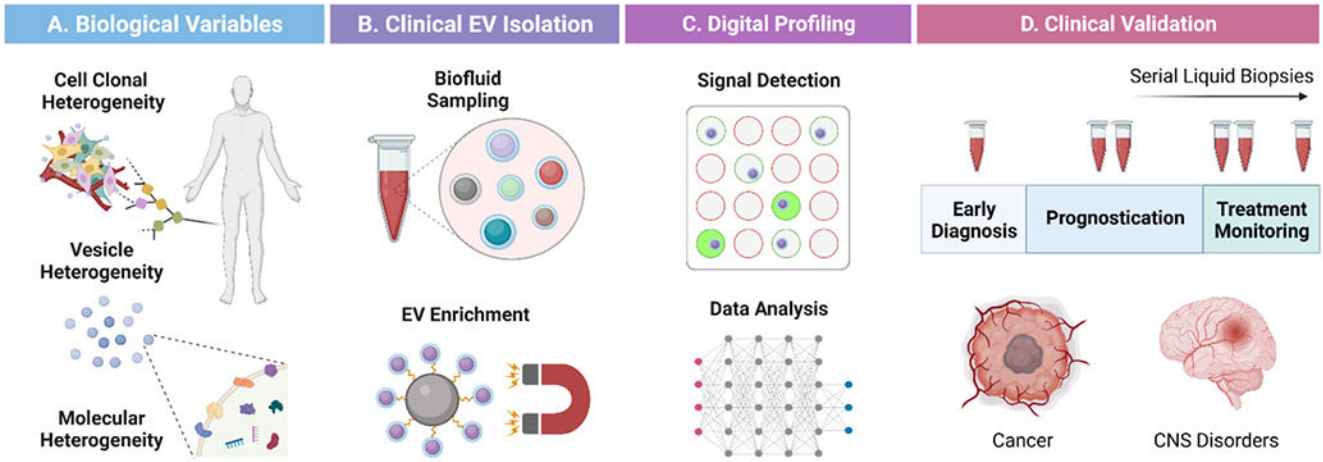

Figure 4.

Clinical translation workflow of digital EV assays. The entire workflow begins by (A) understanding the biological variables of single EVs such as the heterogeneity of their parent cell clones and cell type; the heterogeneity of vesicle size, secretory pathways, and shedding kinetics among each EV; and the heterogeneous molecular content packaged into individual EVs. (B) Clinical biofluids can be readily and serially sampled in a standardized fashion from a patient through minimally invasively sources and materials can be optimized for the selective enrichment of EVs. (C) Digital detection and data analytical tools can be integrated to profile single EV molecular signatures. (D) Digital assays for EV-based liquid biopsies can be clinically validated for a specific context of use—early diagnosis, prognostication, and treatment monitoring for diseases like cancer and CNS disorders.

Table 1.

Summary of Digital EV Assays

class	technique	detection principle	analyte class	LOD[a]	multiplex (*n*)	throughput[b]	ref
Ab–DNA barcoding	BAM	DNA-anchored EVs undergo dPCR *via* isothermal amplification	proteins (GPC1)	N/A	1	moderate	54
	PBA	proximal PBA probe tagged EV, which anneal and amplify as a unique RCA product and is read out *via* sequencing	proteins (Del1, CD151, ITGA1…*n*)	N/A	38	low	57
	seiSEQ	EVs are labeled with Ab–DNA barcodes, amplified by PCR, and are read out *via* sequencing	proteins (CD9, CD11b, CD63…*n*)	N/A	6	low	55
ELIS	Simoa	within microwells, EVs are captured onto microbeads by sandwich Abs and signals detected by fluorescence	proteins (CD9, CD63, EpCAM)	25 EVs/μL	3	moderate	60
	droplet digital ExoELISA	within droplets, EVs are immobilized onto microbeads by sandwich Abs and signals detected by fluorescence	proteins (GPC1, CD63)	10 EVs/μL	2	moderate	62
	DEVA	within droplets, EVs are immobilized onto microbeads by sandwich Abs and signals detected by fluorescence	proteins (CD9, CD63, and CD81)	9 EVs/μL	3	high (20×10^6 droplets/min)	63
PCR	BEAMing dPCR	single-copy RNA is reverse transcribed into cDNA, labeled onto microbeads, conjugated to fluorescent probes, and measured by flow cytometry	nucleic acids (WT *IDH1* G395, mutant *IDH1* A3 95 mRNA)	41 mutant copies/mL	2	moderate	69
	ddPCR	single-copy DNA is extracted from EVs, sorted into droplets, and amplified by PCR for fluorescent readout	nucleic acids (mutant *KRAS* G12V, G12D, G12R DNA)	0.005% mutant allele	7	moderate	18
	TRACER	two aptamer probes in proximity are ligated on a labeled EV and ddPCR is performed	proteins (EpCAM and PD-L1)	0.0735 pg/mL	2	moderate	70
	ExoPLA	two PLA probes are ligated to form a circular DNA for RCA. RCA products are visualized *via* flow cytometry	protein (CD63, CD10, cathepsin B…*n*)	N/A	4	high	75
flow cytometry	single-EV flow cytometry	DNA probes change conformation *via* HCR upon binding to EVs, conjugated with fluorophores that are measured by flow cytometry	proteins (CD63, HER2)	20 μg/mL	2	high	76
	nanoflow cytometry	optics are optimized for EVs with less probe volume, slow flow rates, and specialized detectors	proteins (CD9, CD63, and CD81)	40 nm (size detection limit)	3	high (10^4 particles/min)	78
immunofluorescence imaging	SEA	EVs are immobilized onto a coated glass surface for repeated cycles of immunostaining and imaging	proteins (CD63, EGFRvIII, IDH1-R132…*n*)	N/A	11	low	35
	TIRF	DNAzyme probes bind to miRNAs to produce amplified fluorescence signals detected by TIRF microscopy	nucleic acids (miR-21, miR- 221)	378 copies/μL	2	moderate	80
	NTA	NTA analysis of single EVs by sequentially tracking scattering and fluorescence signals	proteins (CD9, CD63, and CD81)	N/A	3	moderate	82

[a]LOD = limit of detection with each method's unit of measurement.

[b] Throughput is characterized as low, moderate, high (according to length of sample processing and analysis times).